UNIVERSITY OF CALIFORNIA SAN DIEGO

The Design of a Detachable Bronchoscope

A thesis submitted in partial satisfaction of the requirements for a degree of Master of Science

in

Engineering Sciences (Mechanical Engineering)

by

Matthew R. Kohanfars

Committee in charge:

Professor Frank E. Talke, Chair
Professor Vlado Lubarda
Professor Tania Morimoto

2021

The thesis of Matthew R. Kohanfars is approved, and it is acceptable in quality and form for publication on microfilm and electronically.

University of California San Diego
2021

DEDICATION

Dedicated to my beloved parents, my two brothers, my aunt, uncle and their children.

EPIGRAPH

“Few will have the greatness to bend history itself; but each of us can work to change a small portion of events, and in the total of all those acts will be written the history of this generation.”
– Robert F. Kennedy

“Two roads diverged in a wood, and I – I took the one less traveled by, and that has made all the difference.”
– Robert Frost

“The difference between a dreamer and a visionary is that a dreamer has his eyes closed and a visionary has his eyes open.”
– Martin Luther King, Jr

“Success is the ability to go from failure to failure without losing your enthusiasm”
– Winston Churchill

“The cave you fear to enter holds the treasure you seek.”
– Joseph Campbell

"Unless a man is master of his soul, all other kinds of mastery amount to little.”
– Theodore Roosevelt

“There’s a way to do it better – find it.”
– Thomas A. Edison

TABLE OF CONTENTS

LIST OF FIGURES

LIST OF TABLES

ACKNOWLEDGEMENTS

I would like to thank Professor Frank E. Talke for his support as the chair of my committee. His mentorship, support on my thesis work, and master's education has been significant to the development of this work.

I would also like to thank Dr. Farshad Ahadian, for his insightful outlook on engineering science and his feedback on medical devices. His support was critical in the development of the research conducted throughout this thesis.

I want to acknowledge and thank Karcher Morris. His leadership, and forward thinking is an invaluable asset in a medical device research laboratory.

I would also like to acknowledge Yu Li for his many late nights spent in support of the project, and his constant drive to improve the device.

I would also like to thank the rest of the Talke biomedical device laboratory for their research support, perspectives, and feedback. Thank you Rafaela Simones-torigoe, Po-han Chen, Shengfan Hu, Luke Teragan, Allen Hsieh, Benjamin Suen, Oren Gotlib.

Material from this thesis has been published in the 2021ASME ISPS conference on the "Design of a 3D Printed Micro-Transmission System for a Detachable Bronchoscope," by Kohanfars, Matthew; Li, Yu; Morris, Karcher; Ahadian, Farshad; Talke, Frank E.

VITA

2016	Mechanical Engineering Intern, Stone Brewing Co.
2017	Mechanical Engineering Intern, Ultra Communications Inc
2018	B.S. in Mechanical Engineering, University of California San Diego
2018	Minor in Business from Rady School of Management
2018-2021	Graduate Teaching Assistant, University of California San Diego
2018-2021	Graduate Research Assistant, University of California San Diego
2020	Mini MBA from Rady School of Management
2021	Master of Science in Engineering Sciences (Mechanical Engineering)

PRESENTATIONS

Presentation pitch at the University of California Center for Accelerated Innovation Biomedical for a Detachable Bronchoscope for Endotracheal Intubation, Irvine, CA, 2019

Presentation at the Information and Storage Processing Conference for a Detachable Bronchoscope for Endotracheal Intubation, San Diego, CA, 2019

Presentation at the Converge Summer 2020 Incubator Program, University of California San Diego for Rapid Prototyping, San Diego, CA, 2020

ABSTRACT OF THE THESIS

The Design of a Detachable Bronchoscope

by

Matthew R. Kohanfars

Master of Science in Engineering Sciences (Mechanical Engineering)

University of California San Diego, 2021

Professor Frank E. Talke, Chair

In this thesis, 3D printing is employed to prototype a detachable bronchoscope consisting of an articulating arm, a detachment mechanism, a handle with an embedded gearbox, and a micro-transmission located in the arm. The micro-transmission is a novel screw system that converts a rotational degree of freedom from an attached handle to a linear degree of freedom of a moving nut on the screw to a rotational degree of freedom to articulate the distal tip. The design of the screw thread has been analytically and experimentally investigated. The operator's torque input necessary to rotate the distal end of a bronchoscopes linkage system is evaluated with consideration of the forces required to deflect the distal tip. The screw design parameters considered include pitch, thread angle, and material properties. A model has been developed based on screw mechanics equations and the model was confirmed experimentally.

Chapter 1 Introduction to Bronchoscopy

1.1 The Field of Bronchoscopy

A bronchoscope is a medical device that can navigate through the nose or mouth to gain access to a patient's respiratory tract. A typical bronchoscope, as shown in Figure 1, incorporates channels for oxygenation, suction, or procedural biopsies. The distal end of the bronchoscope can be articulated by an operator. The bronchoscope additionally incorporates a light source and a camera lens. These features are typical of the more commonly used bronchoscopes but designs and features vary depending on the manufacturer. A physician can use the bronchoscope's optics, in conjunction with its inherent flexibility, to maneuver through the complex anatomy of a patient's respiratory tract. The respiratory tract is composed of upper and lower segments, both of which are accessible with the use of a bronchoscope. The upper respiratory tract consists of the mouth, nose, nasopharynx, oropharynx, laryngopharynx, and larynx. The lower respiratory tract consists of the trachea, lungs, and the diaphragm (Figure 1).

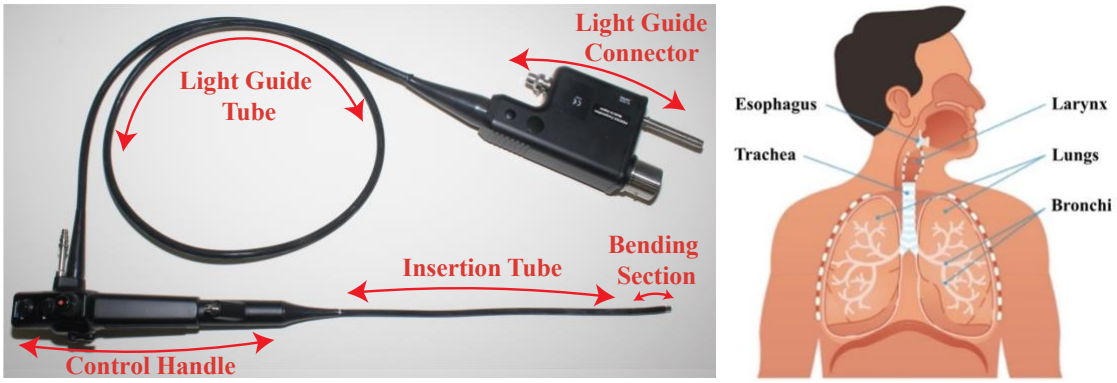

Figure 1: A bronchoscope with annotations of the features of the device (left) and the corresponding anatomical area of focus where the device is typically used (right)[1]

The bronchoscope has uses ranging from foreign body removal, intubation, and treatment of various lung disorders. One common use of the bronchoscope, depicted in Figure 2, is visual navigation of the airway via endoscopic vision. The inserted portion of the scope is positioned at a point of interest, such as a cancer site in the bronchial tree. This allows the physician to utilize the bronchoscope's working channels to take samples, conduct tests, and determine the next steps of patient care.

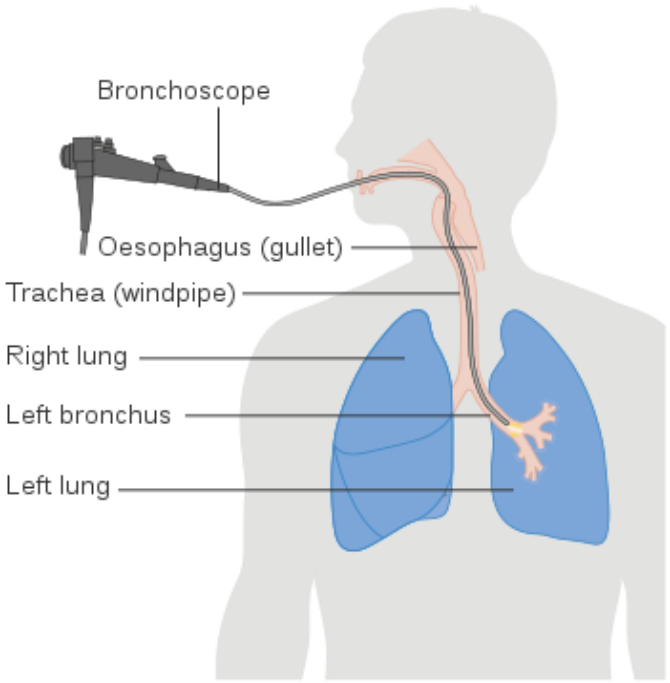

Figure 2: Common use of bronchoscope shown inserted through a patient mouth and navigated into the left lung. Endoscopic vision displays the location on the screen for the operator[2]

1.2 The Unmet Need in Securing a Critical Airway

A bronchoscope is utilized by a few medical specialties: ear, nose, and throat (ENT's), pulmonary medicine, and anesthesiology. For patients that require assistance breathing, a physician within one of these fields may need to perform an intubation. There are approximately 40 million intubations in the United States alone: 36 million intubations occur in the operating

room (OR), 3.2 million intubations occur in the intensive care unit (ICU), and 0.8 million intubations occur in the emergency department as depicted in Figure 3.

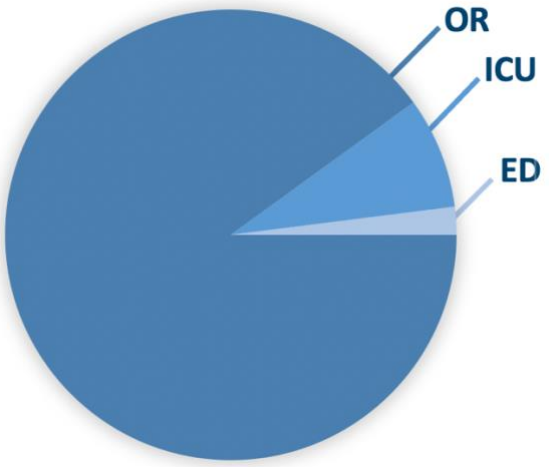

Figure 3: The distribution of intubations conducted annually in the United States

The process of intubation involves inserting an endotracheal tube (ETT) into the patient's airway. However, the anatomy of the airway can complicate the procedure. The physician must first evaluate the airway which involves sizing the tongue, noting the condition of the uvula, gauging the approximate extension of mouth opening, and must assess other potential obstacles such as the presence of teeth [3]. The airway geometry is typically given a Mallampati class from I through IV which corresponds to the level of difficulty of the airway (Figure 4).[4] With a higher Mallampati score, physicians face a greater challenge when it comes to proper placement of the ETT.

If there is a significant delay during intubation (> 4 minutes) and the endotracheal tube cannot be properly placed, then the patient may suffer from permanent brain injury and there may be a loss of life. If complications related to the process of intubation occur and an endotracheal tube needs to be replaced, then the risk of mortality rises substantially.[5] These complications include

issues with endotracheal tube cuff pressure, secretion blockages, incorrect endotracheal tube positioning into the trachea, and improper sizing of the endotracheal tube itself. In

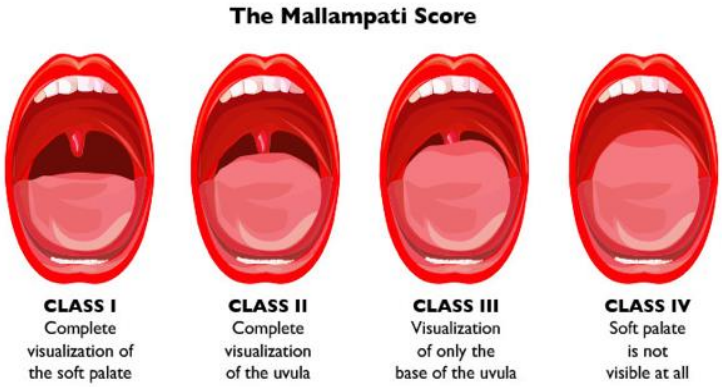

Figure 4: Mallampati Airway Classification (I-IV)[4]

the latter scenarios the intubation tube must be removed and replaced as quickly as possible to regain control of the airway. In critically ill patients, physicians have reported full airway collapses in 1% of all intubation cases. This indicates an urgent need to develop a means to increase the speed and efficiency of intubation in order to prevent an airway disaster.

1.3 Thesis Overview

One option that would mitigate the risk of endotracheal tube replacement is to develop a bronchoscope that maintains a secure and continuous path to the trachea while also allowing a rapid exchange of an endotracheal tube. One potential option that would maintain a continuous airway and expedite the process of endotracheal tube exchange would be to design a detachable bronchoscope. The control handle of the bronchoscope can be detached so that the endotracheal tube can be removed and replaced with a new one. The placement of the new endotracheal tube can be confirmed under endoscopic vision when the control handle is re-attached. In this thesis, the design of a detachable bronchoscope is considered and separated into four individual sub-

systems. These sub-systems include the gearbox, the detachment mechanism, the micro-transmission system, and the distal tip. The gearbox enables the input rotary motion to be converted to an output rotary motion. The detachment system constrains the insertion section of the device, allowing for proper positioning of the transmission system for rotary motion control of the gearbox. The transmission system controls the bending section of the bronchoscope, i.e. the distal tip. This section will be analyzed quantitively and experimentally evaluated. Finally, future work and research directions of the detachable bronchoscope will be discussed.

Chapter 2 State of the Art Technology

2.1 History of Bronchoscopy

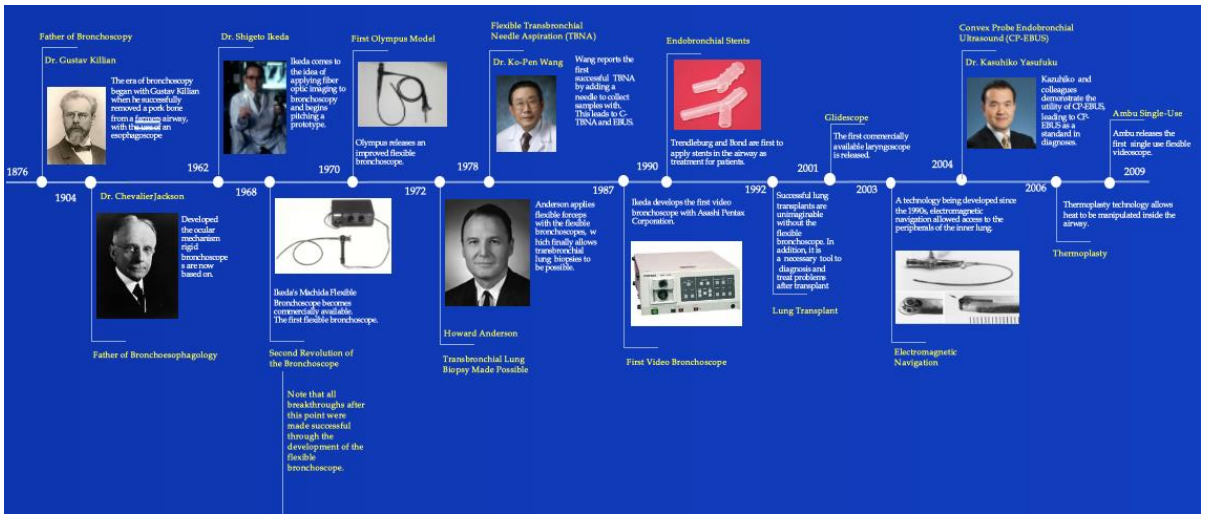

Figure 5: History of bronchoscopy from the initial beginning to the currently used devices.[6-8]

Since the introduction of bronchoscopy, many crucial milestones and prototypes were developed that includes the advancement of videoscopes, electromagnetic navigation scopes, and the latest robotic flexible bronchoscopes.[8] The introduction of bronchoscopy began in 1876 with Gustav Killian (Figure 5), an otolaryngologist considered the father of bronchoscopy. Killian used a rigid bronchoscope to remove a pork bone in a farmer's airway.[7] Following Killian's path, the use of rigid bronchoscopes for direct visualization of the trachea and central airways was adopted by other otolaryngologists. The rigid bronchoscope was used exclusively by ear, nose, and throat (ENT) departments, thoracic surgery assistance, and specialized pulmonology centers up until the 1970's. However, the rigid bronchoscope has inherent limitations, such as not being able to visualize the upper lobes and reaching the distal airways.[8] The development of a flexible apparatus was necessary to eliminate these limitations.

The flexible bronchoscope was a major milestone by Dr. Shigeto Ikeda et al.[7] It was Dr. Ikeda's recognition of the need of a device capable of visualizing lesions and segments of the airway that previous devices were incapable of doing. Dr. Ikeda, a thoracic surgeon and bronchologist, used his experience with airway difficulty to develop the first prototype of a flexible bronchoscope.[8] He used the help of Machida Co. and Olympus Optical Co., to construct several prototypes of flexible bronchoscopes that used fiberoptic bundles as in the company's gastrointestinal fiberscopes. These prototypes consisted of smaller diameters with even more fiberoptic bundles to support visualization, a lightguide, a flexible distal end tip, and an integrated channel for sample collection. The first bronchoscope demonstrated by Ikeda[7] is illustrated in Figure 6. The flexible fiberoptic bronchoscope has since become popular for medical use and, predominantly, the respiratory system.

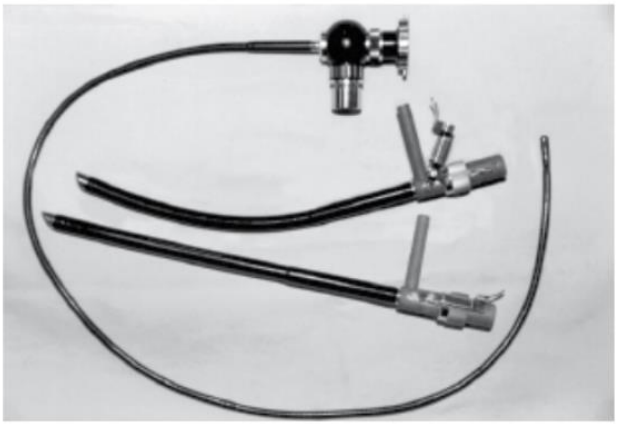

Figure 6: Demonstration of the first bronchoscope prototype developed by Ikeda[7]

Following the invention of the flexible fiberoptic bronchoscope, several enhancements were made that included higher resolution and smaller diameter scopes. The higher resolution bronchoscopes enabled physicians to evaluate and diagnose tracheal surfaces and micro-vessels in more detail.[7] A major breakthrough was the development of Charge Couple Devices (CCD) and

the Complimentary Metal-Oxide Semiconductor (CMOS) camera chips that converted the bronchoscope to a video bronchoscope. The video bronchoscope development was accelerated through the collaboration of Ikeda[7] and the Asahi Pentax corporation (Figure 5).

2.2 Current Medical Technology

Over 100 years after the initial development of the first rigid bronchoscope, bronchoscope devices are now among the most important diagnostics and therapeutics devices in airway medicine[7]. A state of the art flexible bronchoscope is illustrated in Figure 7. It can be separated into four distinct segments: the bronchoscopes control section, the connector section, the insertion section, and the distal end. The bronchoscope *control section is a* handle containing a control knob that maneuvers the distal end of the device. This section includes a port for instruments to be passed through such as forceps for sample collection. The handle of the device has controls for

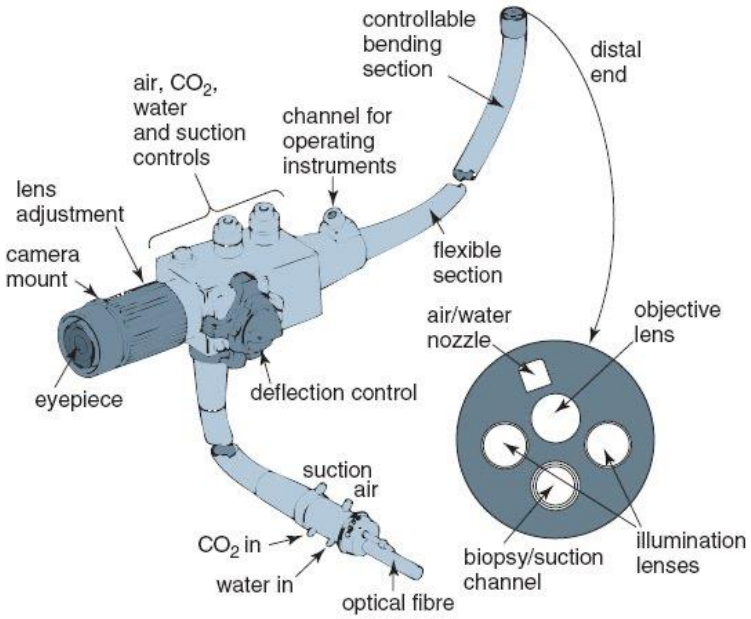

Figure 7: A flexible bronchoscope separated into four distinct segments, the control section, connector section, insertion section and distal end[9]

suction that allows for removal of secretions and to supply fluid for washing or oxygenation support. These controls are only operational when the *connector section* is properly joined with the necessary adapters. The connector section is attached to a separate unit, allowing electrical connections to be made. With the electrical connections performed, the operator can achieve optical support through the light source and optics located at the distal end of the device. The operator can insert the *insertion section* of the device through the airway of a patient and use the vision capabilities of the device to navigate. The insertion section is flexible, allowing the device to slide through complex and curved geometry. To control the direction of the bronchoscope's insertion tube, the *distal end* provides flexion and extension and can be operated from the control sections control knob. Rotation of the distal end (Figure 8) is achieved by an operator thumb movement upwards and downwards on the control knob. Typically, with the movement of the control knob the maximum angles of rotation of a distal end are in the range of $\pm$ 270^{o}. The bending section is able to achieve large angles of rotation due to the linkage mechanism that is illustrated in Figure 8. The linkage system, comprised of a chain and sprocket mechanism, can be manipulated by applying a tension force of the wires (denoted as angulation wires) with the input from the control knob.

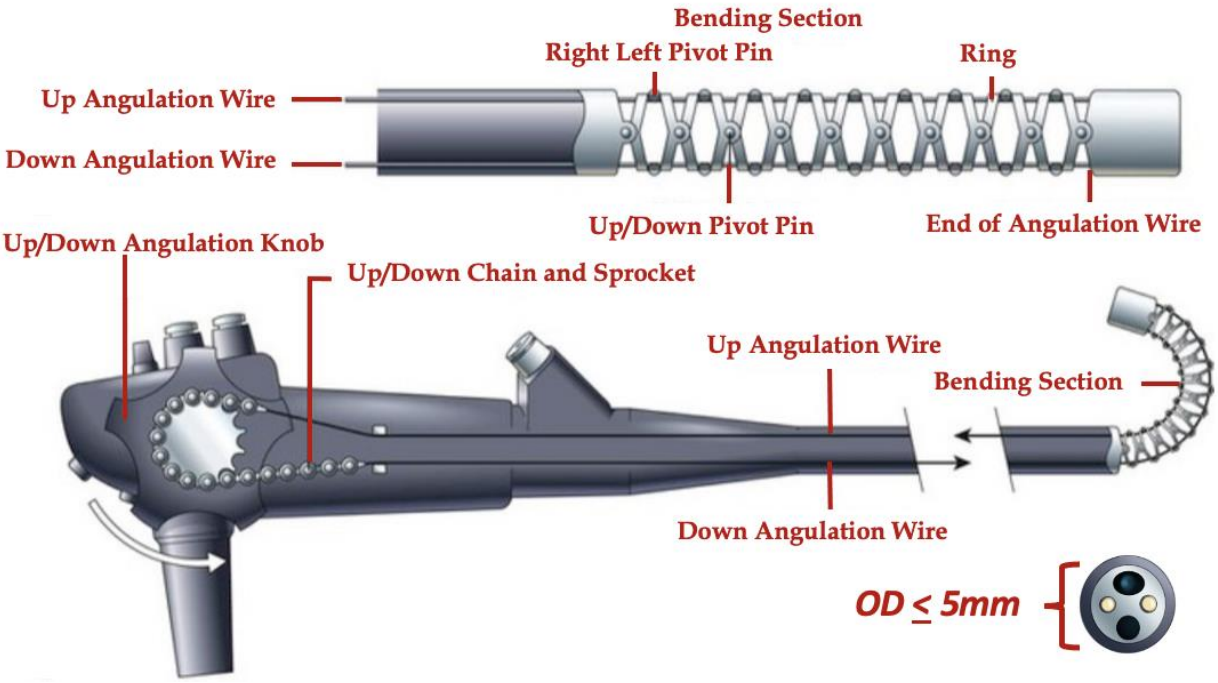

Figure 8: Inside view of a common bronchoscope demonstrating the distal end linkage and angulation wires that are connected to the chain and sprocket system [10]

Typical flexible bronchoscopes used in medical practice range from reusable bronchoscopes to single-use bronchoscopes. The choice of which type is used depends on the medical department innovation executives. Common manufacturers of bronchoscopes are Olympus medical, Pentax, FujiFilm, Karl Storz, Ambu, Verathon Inc., and others. One of the reusable bronchoscopes found in pulmonology departments is the Olympus BF-XT190 (Figure 9) which is considered a therapeutic bronchoscope. In practice, due to its large working channel diameter of 3.2 mm and its ability to rotate the distal end by 120^{o}, the device provides very good suction capability. Additionally, with its excellent optics, a physician can easily diagnose a particular area or visually determine the next steps for patient care. However, these devices must be sterilized after each use in a chemical bath that increases the downtime for the bronchoscope. Hospitals have additionally been concerned over incomplete sanitation of the devices.

Figure 9: Olympus BF-XT190 Therapeutic Flexible Bronchoscope[11]

Due to the major concern over cross contamination of bronchoscopes, several medical device companies have looked into reducing the risk of putting patients in harm's way. Ambu and Verathon have developed single-use bronchoscopes that can be disposed of after each procedural use. One major bronchoscope used by medical professionals is the Ambu aScope™ 4 Broncho Regular, illustrated in Figure 10. The device has a 5.0mm outer diameter, incorporates a 2.2mm working channel with bending capabilities of 180° to 180° while also including functional suction and optical components. Physicians have noted that due to having many of these single-use devices in stock, shortages are not common and patient care can be continuously resumed. However, physicians have stated that it would be desirable to have better control of movement of the distal end and to have better optics in the device. A device with enhanced optics was created by Verathon with their Glidescope bronchoscope. The Glidescope Bflex, illustrated in Figure 11, is known

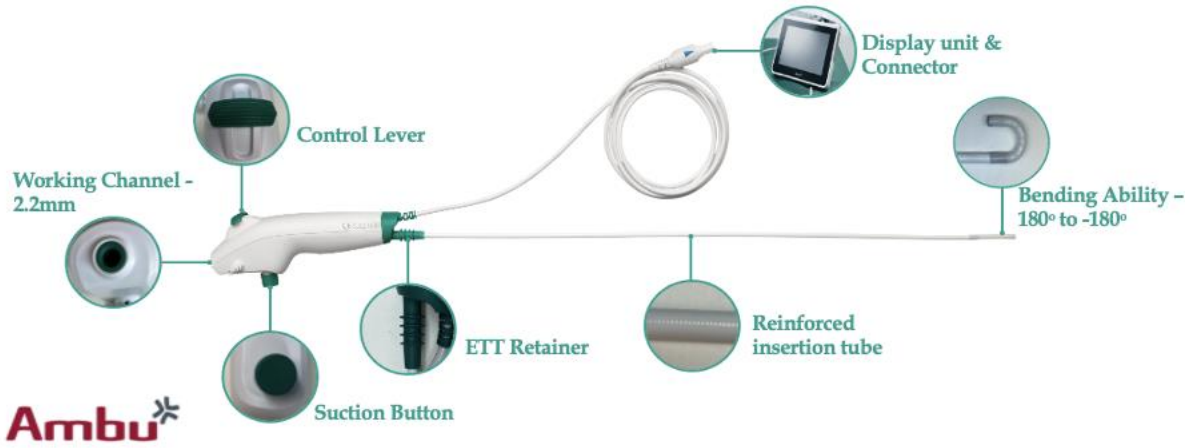

Figure 10: Ambu aScope 4 Broncho Regular Disposable Bronchoscope[12]

for its high-resolution optical output and has similar specifications as the Ambu aScope with a 5.0mm outer diameter and 2.2mm working channel. It additionally incorporates a magnetic QuickConnect™ that removes the need of the long wire that is traditionally seen on bronchoscopes for their optical support. Glidescope also has larger and smaller outer diameter models of 5.8mm and 3.8mm, respectively, for support with varying anatomical airways. It should be noted that Ambu also supports these sized models with these specifications.

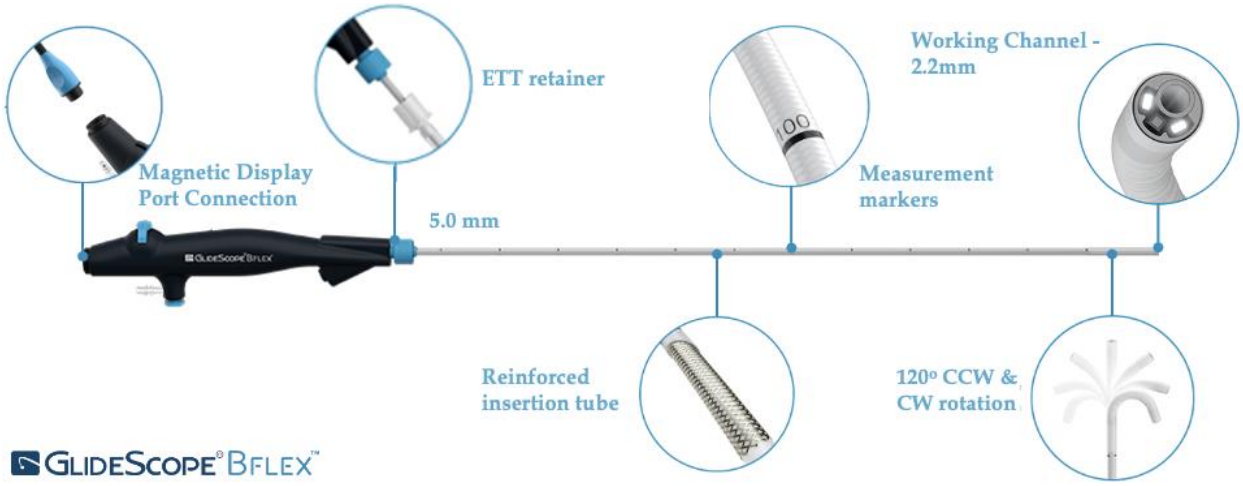

Figure 11: Glidescope BFlex single-use bronchoscope developed by Verathon.[13]

2.3 Future of Bronchoscopy

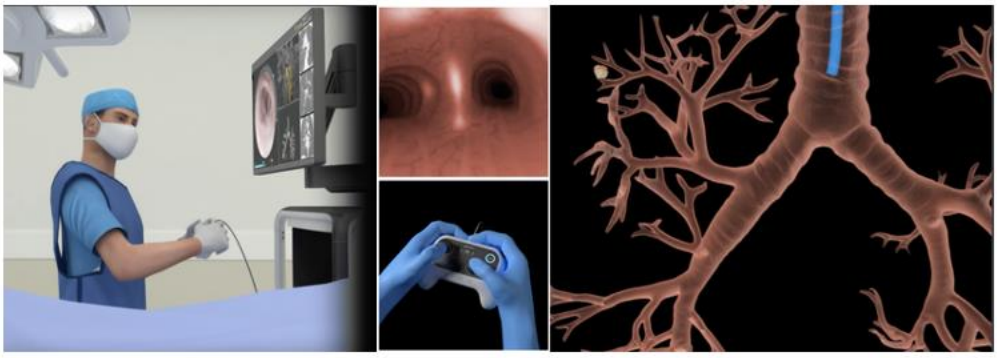

Figure 12: Monarch endoscopy device that allows for movement of the bronchoscopes flexible portion through the airway by the input from a controller.[14]

The future of bronchoscopy is towards developing with new and improved products that can assist physicians and improve the medical procedures conducted. Several indications allow for a clear path of the future of advancing flexible bronchoscopes. Physicians require several main characteristics of a typical flexible bronchoscope. These are great optics, control, and outstanding reliability. The optics of a bronchoscope will continue to improve, as better resolution of optical displays and light emitting diodes will be incorporated in future devices. Flexible bronchoscopes will have better maneuverability and control as depicted in Figure 12 with the Monarch endoscopy platform. This platform illustrates the precision control of the flexible portion of a bronchoscope via a controller. The operator of the device can navigate the respiratory system with a high degree of accuracy by controlling the robotic system through teleoperation. The device uses a magnet that is located outside of the patient to control the movement of the bronchoscope through the anatomy. As the operator utilizes the joysticks of the controller, the magnet will accurately move to the desired location causing the inserted flexible portion to follow.

Maintaining the control of the distal end system is vital in operating an endoscope. Many different designs techniques have been used to deviate from the conventional endoscope pulley

system. Garben et al.[15] have developed a disposable endoscope that has a piston driven actuator to rotate the distal end of the system. The rubber bellows, illustrated in Figure 13, begin their motion by filling the pressure lines causing the distal end to rotate. To precisely control the position, an electromechanical system that connects to the bellow pressure lines has been

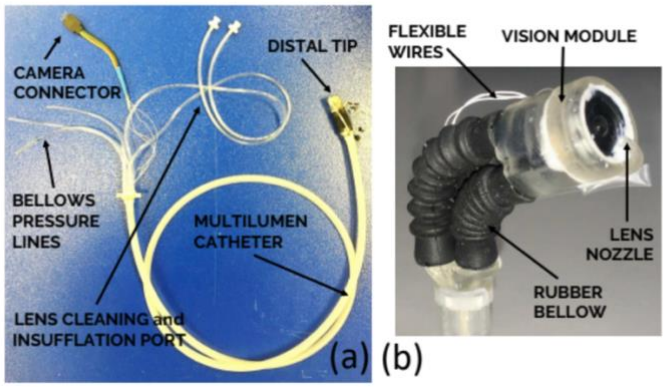

Figure 13: (a) A pneumatically controlled endoscope with its components annotated (b) a direct view of the endoscopes distal end with rubber bellows shown.[15]

developed.[15]. Chen et al.[16] developed a prototype of a motor driven endoscope. The motor is located at the distal end of the endoscope and eliminates the need for the wire to span through the entire length of the endoscope. The drive system, commonly known as a capstan driven, has two wires wound in opposite directions on a shaft allowing for the motor rotation to change the displacement of the wire to cause motion of the distal end. Motors to control endoscopes are becoming more common. To reduce the size of the motors, micromotors have been developed to minimize the space utilized inside an endoscope.

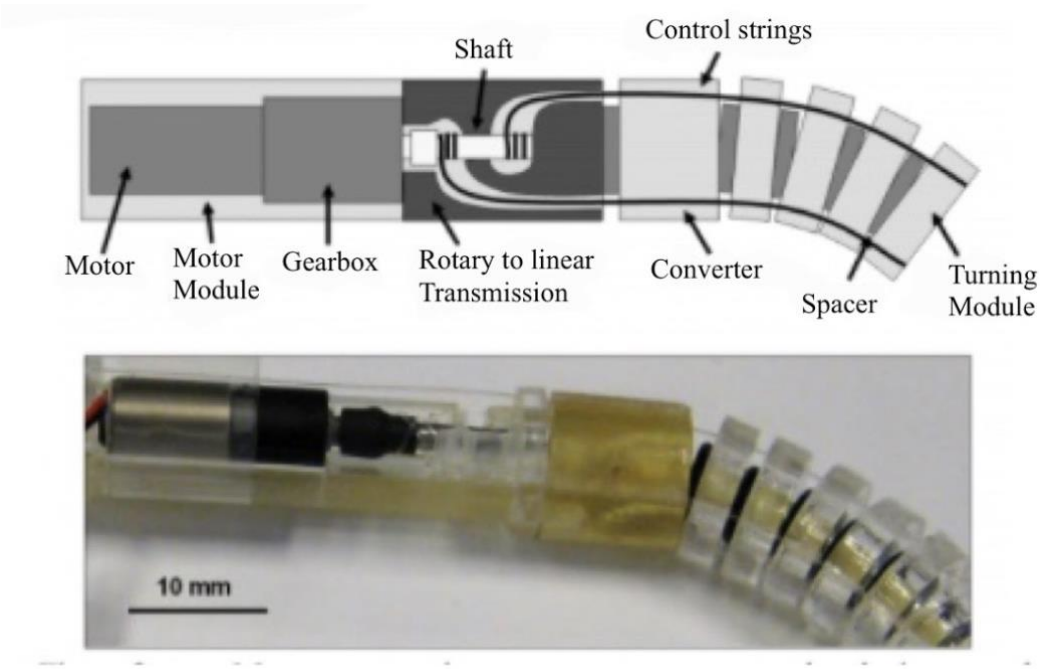

Figure 14: A disposable endoscope prototype that is actuated with motors inside the body. The motor (located at the distal portion) controls a capstan drive that causes the motion of the linkage system.[16]

2.4 Detachment Mechanisms

Rapid connection and detachment mechanisms have become a vital engineering application in many fields and have particularly grown with medical device development. Medical inventions rely on detachment systems to be reliable, quickly decouplable or recoupable, and providing a secure connection without failure. Medical innovations such as the Penumbra Coil 400^{TM}, a device used to treat endovascular aneurysms by delivering a coiled wire to the delivery location, can expedite procedures by using a detachable system. The detachment mechanism of this device is illustrated in Figure 15. A nitinol stretch wire is used to remain in tension while the coils can be released into the aneurysm sac of the target location.[17] With the coils released, the system can decouple from the nitinol wire by the upward movement of the lever on the detachment handle. The decoupling occurs in the detachment tip (Figure 15), where the pull wire keeps the system in

place. With the movement of the lever, the pull wires force is relieved, causing the release of the coil leading to a separation from the treatment wire and handle.

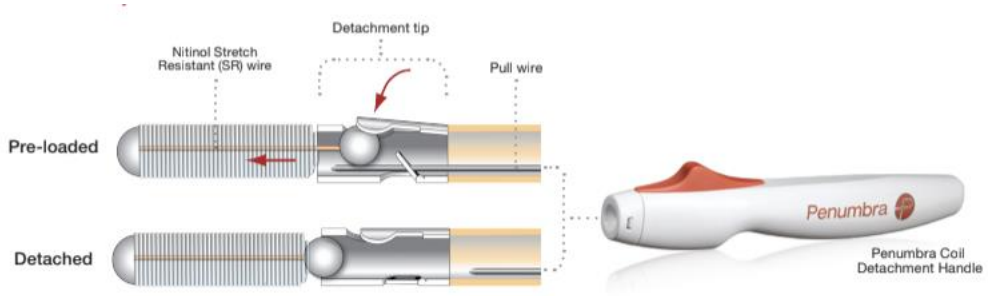

Figure 12: The Prenumbra Coil 400^{TM} is a detachable brain aneurysm device capable of unloading nitinol wire into a target location by disconnecting the Prenumbra coil detachment handle from the stretch resistant wire.[17]

Moreover, with the detachment, the handle of the device can be disposed of eliminating the concern over cross-contaminating from patient to patient.

Detachment systems have also impacted other fields of medicine that relate to surgical and endoscopic devices. These detachment systems can be seen in forceps devices that are typically used to hold tissue, collect samples, or move obstructions in anatomical cavities. The commonly used endoscopic instrument shown in Figure 16 has the connection made from the actuating handle to the ball and socket on the actuation rod. To fully couple the device, a threaded knob insert is rotated until the engagement of a section cutout on the actuation rod is made for a friction fit. When connected the actuating handle can be used to manually manipulate the forceps, causing either a rotational or pivotal movement of the end-effector based on the operator's control.[18]

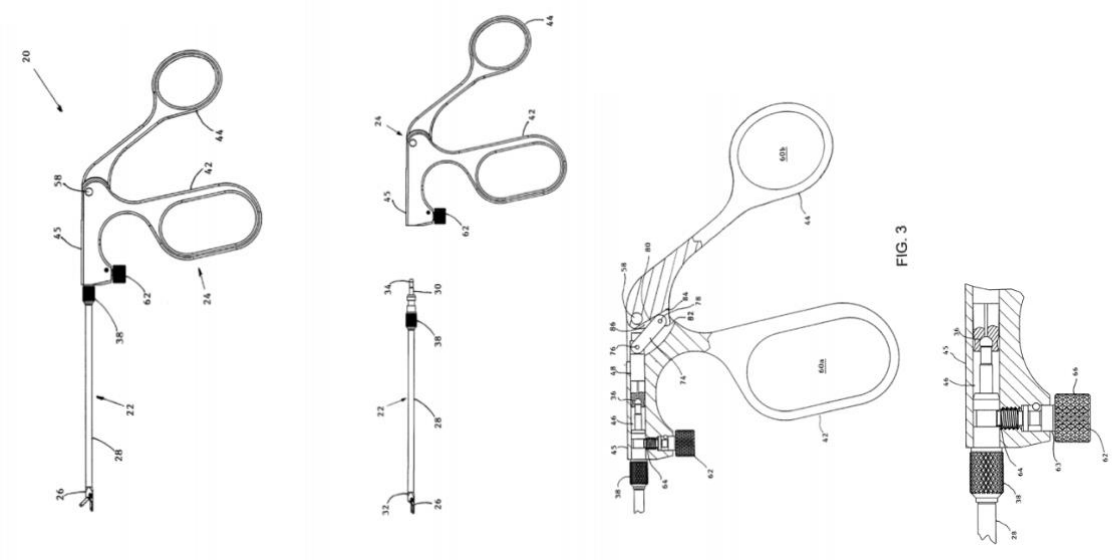

Figure 16: Forceps attached to a handle that allows for movement of the distal end. The system is connected by a threaded knob insert (see 62) that allows for the forceps to be engaged to the handle. The threaded knob can then be rotated in the counterclockwise rotation to disconnect the forceps system.[18]

With endoscopic devices being heavily relied on for assisting in surgery and examination it has become a great area for medical device innovation. In several previously patented art, depictions of creating a detachable mechanism to be incorporated within an endoscope has been illustrated (Figure 17 & Figure 18). As shown in Figure 17, the elongation portion of the device can be detached with a disconnection from a shaft and light guide. This allows the operator to disconnect the elongated portion of the device to potentially attach a new, different sized (length or diameter), or repaired section when necessary.[19] As a result of the connection from the handle to the elongated portion, in this device the physician aligns the light source, visual element, and the handles gear system to activate the maneuverability of the distal end. For example, in procedures that require usage of a bronchoscope with different diameters such as an initial bronchial lavage (larger diameter channel of a bronchoscope needed) can follow with a smaller diameter through the airway if necessary. This will allow physicians to maintain one control handle, with the option of using of different insertion sections, thereby reducing the total amount

of endoscopes needed during one procedure. Additionally, detachment mechanisms incorporated in endoscopic devices will be complimentary in training medical practitioners. With training that places physicians with differing airway scenarios (i.e. Mallampati scores from I-IV), such a device capable of changing elongated portions are ideal for learning the devices capabilities.

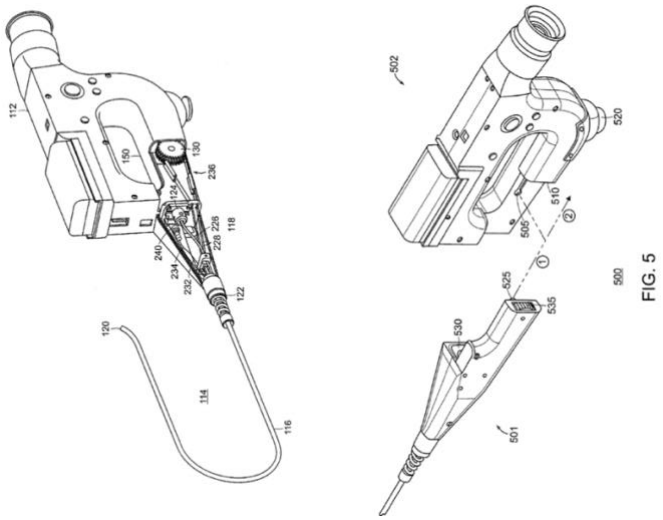

Figure 17: Prior art of a detachable endoscope system with the fully connected assembly (on left) shown and the handle disconnected from the insertion section of the device (on right).[19]

Although the use of the above detachable endoscopes can be incorporated in many medical procedures, one obvious limitation is the actual detachment design. The elongated portion requires that the physician aligns the proximal segment through a hole located on the handle and then pushing down on the control handle to lock the two components together. The proximal segment of the elongated portion is bulky, creating a much greater diameter overall and ultimately becomes challenging to connect the two components together easily. In Figure 18, another detachable endoscope design is illustrated. In this design developed by Krupa et al,[19] the handle can be decoupled from the insertion section by twisting the insertion section aligning the tongue and groove detachment. When secure connection of the insertion section and control handle are made (Figure 18 on the right) the ability to maneuver the distal end can now be connected by lifting 10

and placing it over 23. This enables the operator to articulate the distal end linkage of the endoscope. With this current design, there are multiple steps in connecting the system by initially aligning the detachment system then following with the connection of the articulation wire. Additionally, the detachment system significantly increases the diameter of the insertion tube and is difficult to use. From the detachable systems discussed above, it is apparent that a mechanism is desirable that is reliable and simple to use, while also quickly to connect or disconnect.

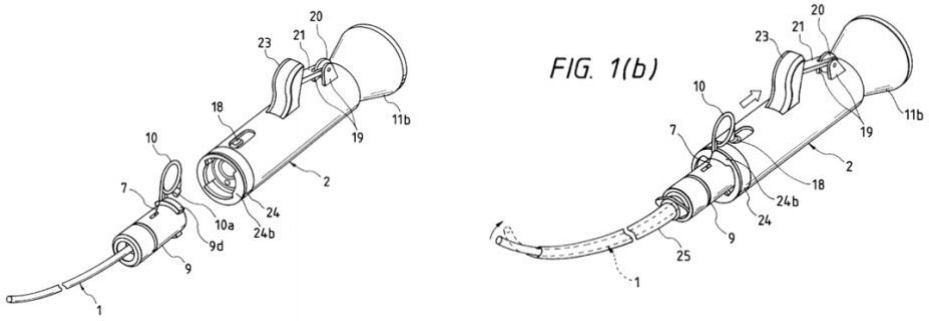

Figure 18: A detachable endoscope with the system disconnected (on left) and connected system (on right). The disconnected portion illustrates the area of the insertion tube that must align with the location on the control handle. When aligned properly the system is fully connected.[20]

Chapter 3: Fundamentals of Screw and Gear Design

3.1 Introduction

The goal of this thesis is to design a detachable bronchoscope that allows the separation and reattachment of the flexible insertion tube from the handle of the device. The design chosen for this task uses a counterclockwise and clockwise threaded screw mechanism located inside the insertion tube that activates the rotation of the bending section. A gear train is positioned in the handle to transform the input motion of a lever on the handle into a rotary output motion to initiate the rotation of the screw. This chapter discusses the fundamentals of screw and gear design in the implementation of a detachable bronchoscope.

3.2 Screw Fundamentals

In robotics, the connection of different manipulations, also known as links, is made possible through its joints, which allow the links to travel in various types of movement. Typical joints and links like the ones illustrated in Figure 19 are the major types used in mechanical design that allow for modes of travel. Our search for the joint movement narrows with the helical joint depicted in Figure 19. The helical or screw joint will complement our design by translating the force from the input of the operator into movement at the detachable bronchoscope's distal end. This joint is also applicable to other medical products and detachable devices.

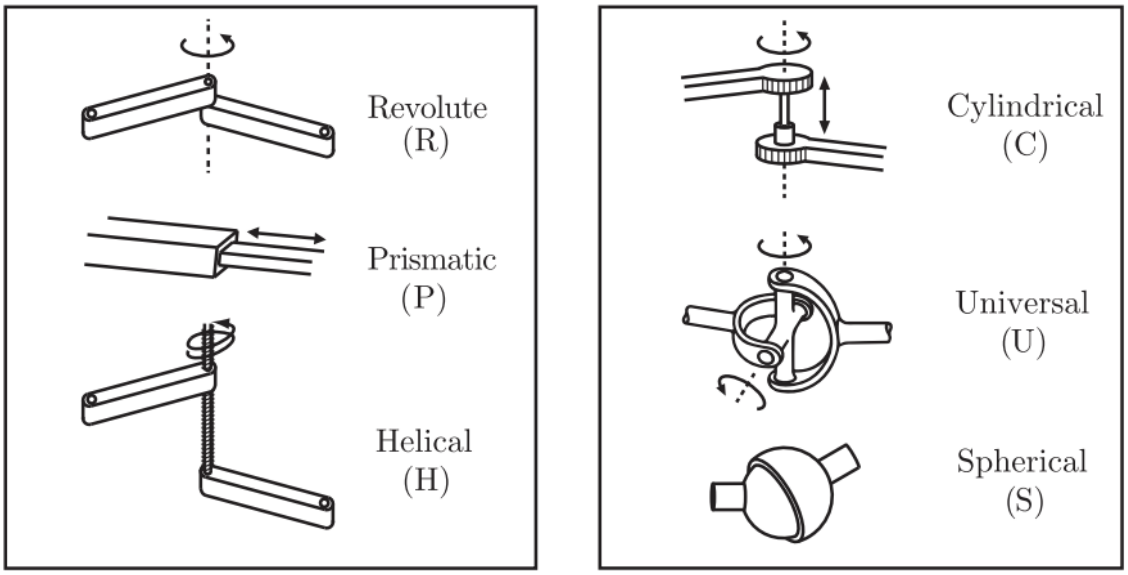

Figure 19: Common joints used in robotics with depiction of a revolute, prismatic, helical, cylindrical, universal and spherical joint.[21]

The screw joint allows the conversion of a rotational motion into a translational motion or, equivalently, an axial force. The helical wrapping around the cylindrical base of a screw is called the screw thread. The thread wrapping is either right-handed (clockwise) or left-handed (counterclockwise). Depending on whether the thread wraps around the screw in a clockwise or counterclockwise direction, the linear translation of the screw will be directed towards or away from the rotational input torque. This is a significant design feature of a screw. Screw thread modification can involve the screw angle or screw pitch changes. For example, increasing the pitch increases the distance traveled by the nut along the screw for a given torque input. This can have implications in torque efficiency and power analysis for a system, which will be discussed in later sections.

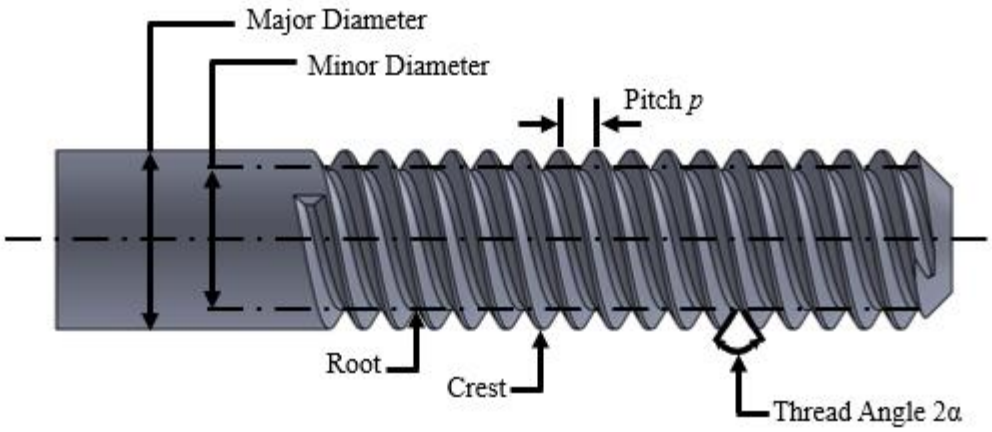

Figure 20: Illustration of a screw joint with annotated terminology

In order to discuss the mechanics of a screw, its terminology must be understood. The general characteristics of a screw are illustrated in Figure 20. In order to express a relationship between the joint's rotation and translation of an object on the screw, such as a nut, the meaning of pitch must be defined. The pitch, as Ball[22] defines it, is a "rectilinear distance which the nut moves along the screw as the nut is rotated through an angular unit of circular measure." The pitch is therefore defined as the distance from a point on the screw thread to a corresponding point on the next thread. This is calculated by dividing the length of the screw by the number of threads. To determine the distance traveled by the nut per one revolution, we must introduce the lead of the screw. The lead of the screw is equal to the pitch of the screw in a single start thread. That is, when the screw advances one complete turn (a nut rotation of 360^{o}), the distance the nut has traversed is equal to the distance of the pitch.

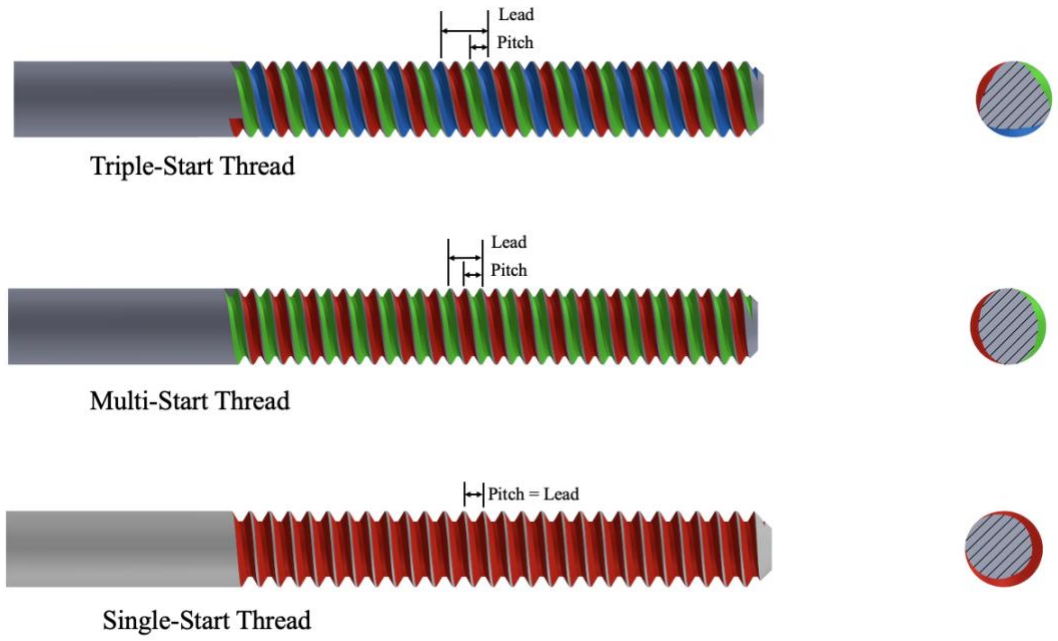

Figure 21: Interlaced threads on a screw depicted with comparison to a single-started thread. Front view of the screw shown to illustrate the starting front geometry of the screw thread.

This is different with a thread that has multiple starts where the threads are intertwined with one another, as depicted in Figure 21. The interwoven threads cause the lead (l) to be equal to the pitch (p) multiplied by the number of interlaced threads.

$$l = \#\ of\ starts * p \quad \text{(Equation 1)}$$

There are many advantages of using interlaced threads such as the increased contact surface area that is present in a thread rotation.[23] Moreover, in a screw that uses interlaced threads, there is an increase in the lead distance without a change in the pitch. Consequently, the linear traversal along a screw can then be represented by the angle of rotation yielded by the input of a torque F_τ, and the lead of the screw l:

$$Distance\ Traversed = x = l\frac{\theta}{2\pi} = ln_t \qquad \text{(Equation 2)}$$

The above equation indicates that the distance the nut travels along a thread is proportional to the lead of the screw l and the number of rotations n_t.

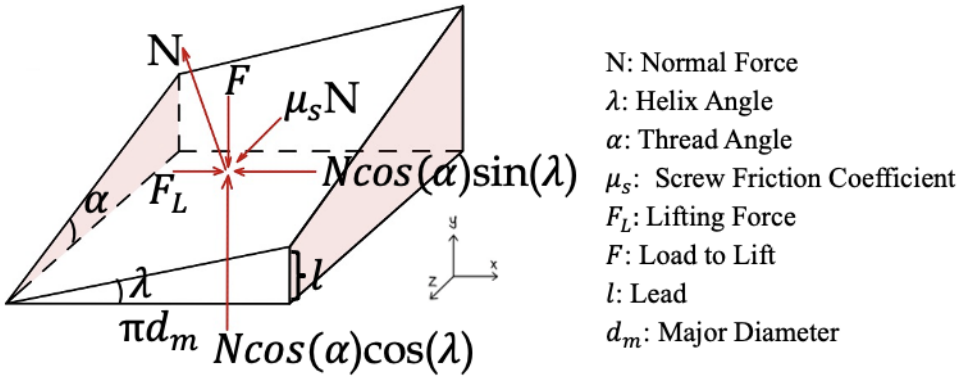

Figure 22: Geometrical representation of a section of a screw thread shown as a wedge with associated forces in question noted.

When a torque input is applied to a screw, the associated loads can be mathematically determined. To analyze this, a section of the thread can be separated and taken as the wedge illustrated in Figure 22. In this Figure, the lead or helical

angle (λ) of the thread is the angle that represents the constant rotation or helical path of a thread. This angle can be explicitly shown by the relationship between the lead distance and the major diameter of the screw:

$$\lambda = arctan(\frac{l}{\pi d_m}) \qquad \text{(Equation 3)}$$

This relationship shows that the base of the triangle is formed by the circumference of the screw shaft with the right portion of the screw thread being the lead. The hypotenuse of the triangle forms the path that the length of the nut takes along the helical thread. Increasing the helix angle will increase the incline of the thread, which is indicative of a larder lead distance for the screw. From this result it can be noted that as the diameter of the screw shrinks, the lead angle must be increased to maintain a constant lead distance. Depending on the helix angle,

the lifting force F_L can be determined. From Figure 22 the following static equilibrium equations can be obtained from the free body diagram:

$$\sum F_x = F_L - \mu_s N cos(\lambda) - N cos(\alpha) sin(\lambda) = 0 \qquad \text{(Equation 4)}$$

$$\sum F_y = N cos(\alpha) cos(\lambda) - \mu_s N sin(\lambda) - F = 0 \qquad \text{(Equation 5)}$$

where μ_s is the coefficient of static friction, α the thread angle, N the normal force applied at an angle λ, and F the load of the nut being lifted. From equations 3 and 4, we obtain F_L as

$$F_L = \frac{F(cos(\alpha) sin(\lambda) + \mu_s cos(\lambda))}{cos(\alpha) cos(\lambda) - \mu_s sin(\lambda)} \qquad \text{(Equation 6)}$$

Dividing by $cos(\lambda)$, we obtain

$$F_L = \frac{F(cos(\alpha) tan(\lambda) + \mu_s)}{cos(\alpha) - \mu_s tan(\lambda)} \qquad \text{(Equation 7)}$$

Equation 7 can be simplified further using the definition of the lead angle relationship from equation 3, resulting in

$$F_L = \frac{F(l - \mu_s \pi d_m sec(\alpha))}{\pi d_m - \mu_s l sec(\alpha)} \qquad \text{(Equation 8)}$$

Equation 8 shows the effect of the lead distance l and its effect on the force required to lift a load. The larger the lead distance with respect to a fixed force F would require a higher lifting force F_L. In many cases, the torque needed to raise a load is of importance. Considering that the perpendicular distance from the center of the shaft to the nut on a screw is the radial distance, $\frac{d_m}{2}$, the torque, τ_L, is determined by

$$\tau_L = F_L \frac{d_m}{2} \qquad \text{(Equation 9)}$$

The above equation can be used to estimate the torque or twisting force required to lift a nut along a screw shaft.

The conversion of a rotational input to a linear translation along a screw shaft is defined as the efficiency of a screw. The efficiency depends on numerous factors that affect the

performance of screws' ability to convert this rotation to a translation along a shaft. Main efficiency dependencies are on the helix angle, lead distance, frictional forces, and the torque input. The efficiency can be thought of as the ratio between power out and power in, which in terms of a screw system is

$$\eta_{efficiency} = \frac{Fl}{2\pi\tau_L} \qquad \text{(Equation 10)}$$

The efficiency can be put in terms of our previous equations to show the dependency on the coefficient of friction, the helix angle, and the thread angle of the screw thread. This relationship is

$$\eta_{efficiency} = \frac{1-\mu_s tan(\lambda) sec(\alpha)}{tan(\lambda) + \mu_s sec(\alpha)} \qquad \text{(Equation 11)}$$

Due to its ease of manufacturability, a commonly used screw thread is the Acme thread form which has a trapezoidal profile with thread angle $\alpha = 14.5^o$. The efficiency of the Acme thread calculated in equation 11 can be determined by applying different materials to determine the efficiency plot as a function of the helix angle. In Table 1, the coefficient of static friction is shown, for typical, 3D printed materials. Additional materials were also analyzed (Figure 23), to determine the effect of the helix angle on screw efficiency. We observed from Figure 23 that the efficiency for an Acme thread can reach up to 70%.

Table 1: Material for screws and the corresponding coefficient of static friction[28-29].

Material	Coefficient of Static Friction (μ)
Formlabs - Durable | Durable	0.32
Formlabs - Tough | Tough	0.77
Formlabs - Durable | Tough	0.16
Aluminum | Aluminum	1.20
Auminum-Bronze | Steel	0.45
Nylon | Nylon	0.20
Nylon | Steel	0.40

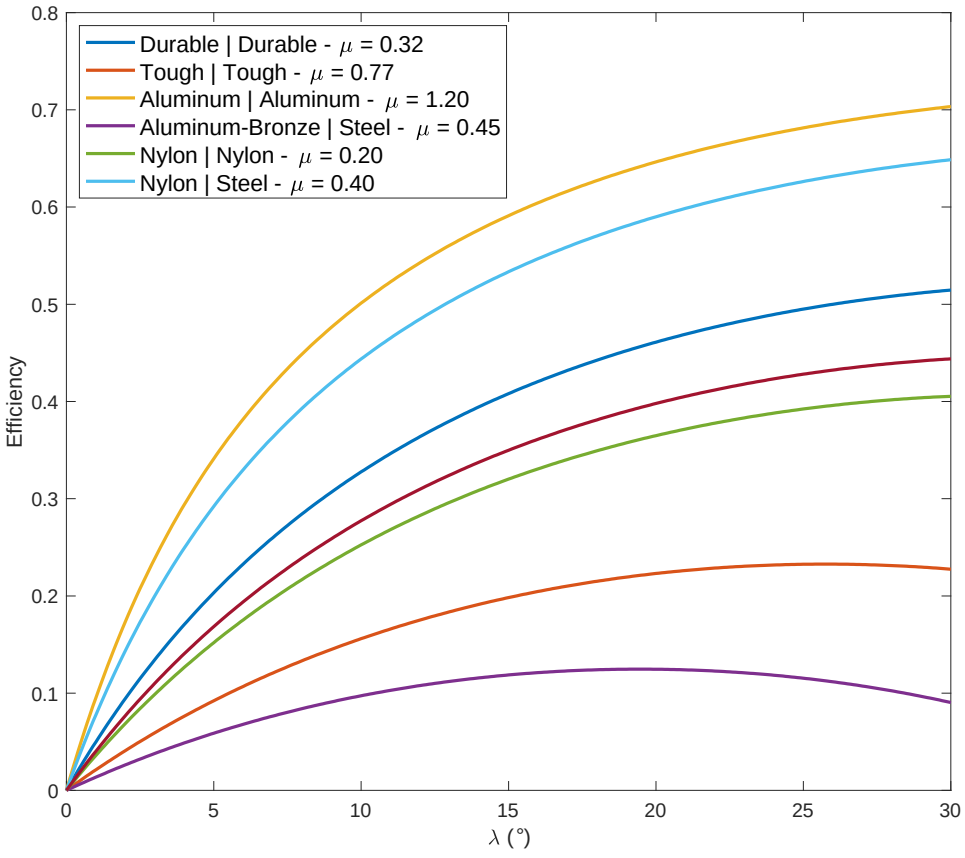

Figure 23: Screw efficiency versus lead angle lambda for an Acme thread profile

The efficiency to convert rotational motion to translational motion depends on the actual design. If a collar is added to the screw to provide support, the screw efficiency will change (Figure 24).

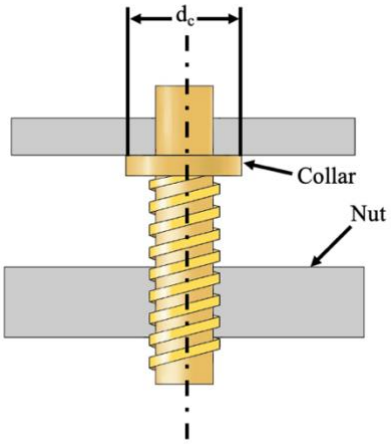

Figure 24: A screw and collar system illustrated to depict the mechanics of a screw system with a common constraint.

In this case the torque is given by

$$\tau_{LC} = F_L \frac{d_m}{2} + F_L \frac{\mu_C d_c}{2} \qquad \text{(Equation 12)}$$

Where μ_C is the coefficient of static friction of the collar and d_C the diameter of the screw collar.

The efficiency with respect to the friction of the collar becomes

$$\eta_{efficiency} = \frac{1-\mu tan(\lambda)sec(\alpha)}{1+\mu cot(\lambda)sec(\alpha)+\mu_c \frac{dc}{dm}(cot(\lambda)+\mu sec(\alpha))} \qquad \text{(Equation 13)}$$

3.3 Gear Systems

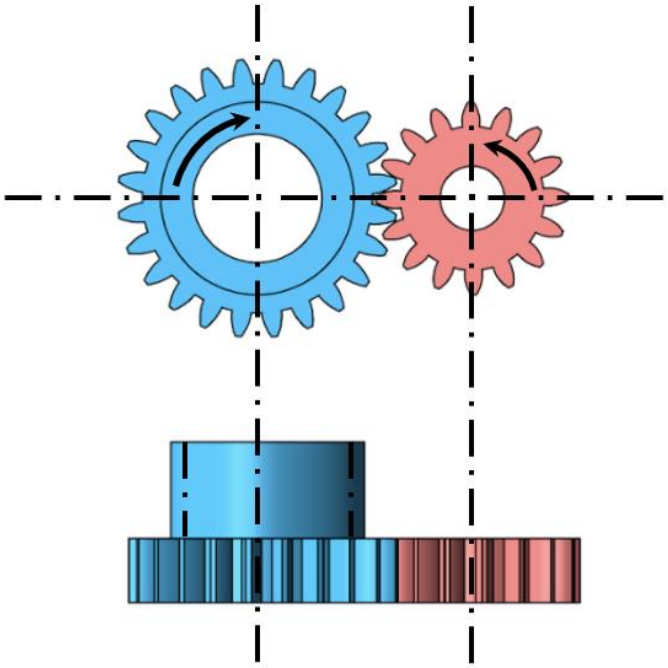

Figure 25: Spur gear representation with parallel axes of rotation shown

In this section gear systems are described relating to the geometry and force transmission for spur and bevel gears. In a gear system force and motion is transmitted through the movement of gears that have their teeth meshed together. The meshing of gears provides a torsional moment and the transmission of power from the input gear to the output gear. A typical gear used to transmit motion is a spur gear that is shown in Figure 25. Spur gears are the simplest gears due to their ability to transmit motion from one parallel shaft to another parallel shaft. Spur gears are prominent in many applications that range from automotive components to medical devices. Another commonly gear used to transmit motion is a bevel gear that transfers rotary motion between intersecting lines (Figure 26).

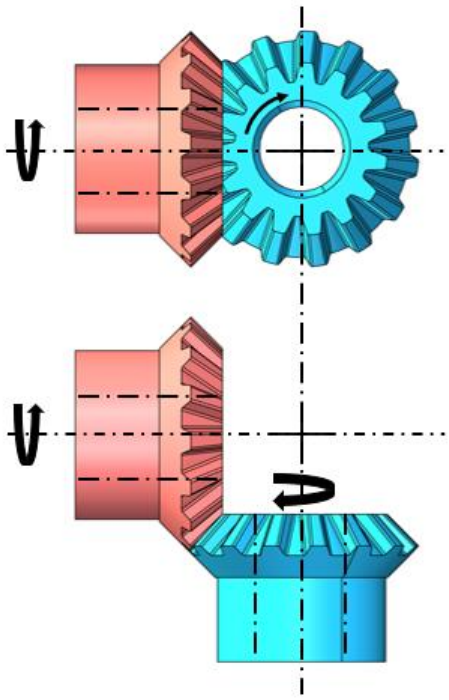

Figure 23: Bevel gear setup illustrated with rotational axes depicted

By utilizing a bevel gear, the input motion can be transmitted perpendicularly allowing for a direction of motion change in a gear system. In order to understand the motion of gears terminology must be defined. In a sequence of gears meshed together, the gear with the smaller number of teeth is called a pinion and the larger of the two called the gear.[26] With the terms in Figure 27 the following are detailed:

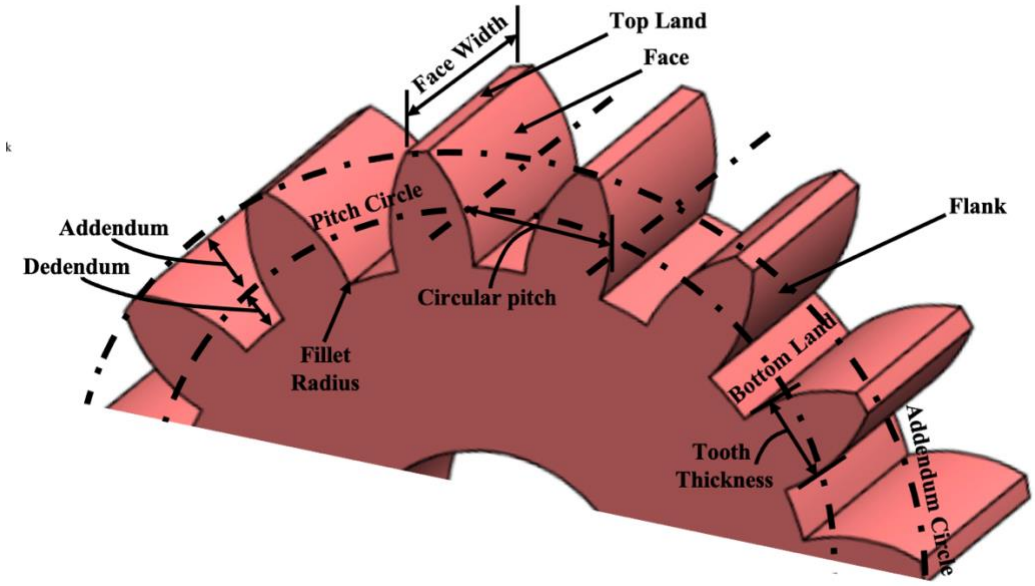

Figure 24: Annotated spur gear slice.

The *pitch circle* of a gear is the circle that is derived from the number set of teeth and the diametrical pitch of the gear where the diametrical pitch is the ratio of number of teeth to the pitch diameter. The diametrical pitch in equation form is defined as

$$P_d = \frac{N_t}{d_p}$$

The pitch circle is the theoretical circle on which all calculations are typically based.[26] *Circular pitch* of a gear is the distance along one point on a gear tooth to another adjacent point measured across the pitch circle. The summing of the *tooth thickness* and width of space between neighboring teeth gives the circular pitch. The circular pitch is determined from the following equation where d_P the pitch diameter:

$$P_c = \frac{\pi}{d_p}$$

The *module (m)* of the gear is a ratio of the pitch diameter to the number of teeth of a gear.[26] This is the indication of how big or small a gear will be. This can be calculated by the following equation

$$Module(m) = \frac{d_P}{N_t}$$

Where N_t is the number of teeth of the gear.

Calculations of gear systems are based upon the pitch circle. These calculations can be depicted in a typical spur gear setup between the forces generated from the pinion and the gear illustrated in Figure 28. In Figure 28 the force from the gear on the pinion is separated

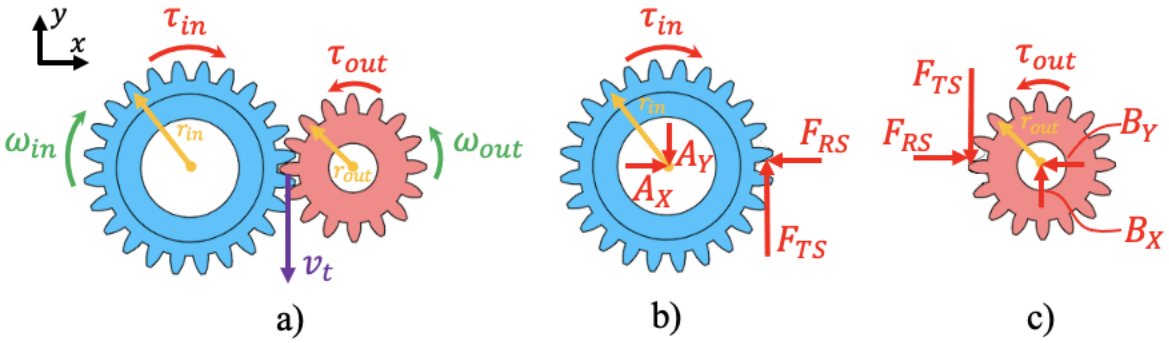

Figure 28: (a) Spur gears meshed together with torque represented along with angular velocity directions (b) Associated forces and torques shown on spur gear (c) Associated forces and torques shown on spur pinion

in two components, F_{TS} and F_{RS}, representing the tangential and radial component of the forces, respectively. The tangential component of the gear is tangent to the pitch circle of the gear and therefore transmits the torque between the gears. The radial force generates a load. The pinion also experiences reaction forces at the pinned joint and is depicted in Figure 28 as A_X and A_Y. Additionally, there is an input torque which is shown as τ_{in}. The torque, τ_{in}, is usually generated from a motor, direct rotational input from a user, or another torque source. The gear with a torque output is illustrated in Figure 28. The gear experiences equal but opposite forces, F_{TS} and F_{RS}. Similarly, this gear is pinned about its center and experience's reaction forces noted by B_X and B_Y.

The output torque of the system is listed in Figure 28 (c) as τ_{out}. By evaluating the two above systems, Figure 28 (b) and (c), the sum of the moment equations about the center pinned joints are

$$\sum M_O = -\tau_{in} + r_{in}F_{TS} = 0 \text{ and}$$

$$\sum M_P = -\tau_{out} + r_{out}F_{TS} = 0$$

From the above equations, we can determine the output torque of our spur gear system

$$\tau_{out} = \frac{r_{out}}{r_{in}}\tau_{in}$$

This demonstrates how torque depends on the gear sizes, and by altering the size of the gear radii with the same input torque, the output torque can be amplified. An important property of gear systems is mechanical advantage, which is a measure of the total output amplification of a given system. In this spur gear system, the mechanical advantage is

$$M.A. = \frac{\tau_{out}}{\tau_{in}} = \frac{r_{out}}{r_{in}}$$

From the above relationship of the mechanical advantage, the ratio of the output torque versus input torque is explicitly shown as the ratio of the gear systems radii. A similar evaluation of the forces, torques, and mechanical advantage can be done for a set of bevel gears. In Figure 29, the forces associated with a bevel gear are illustrated with the top view of the bevel gear shown for clarity. The forces associated with the bevel gear is a tangential, radial, and axial component noted as F_{TB}, F_{RB}, F_{AB}, respectively. These results will become significant in the calculations for the gearbox utilized in the detachable bronchoscope design.

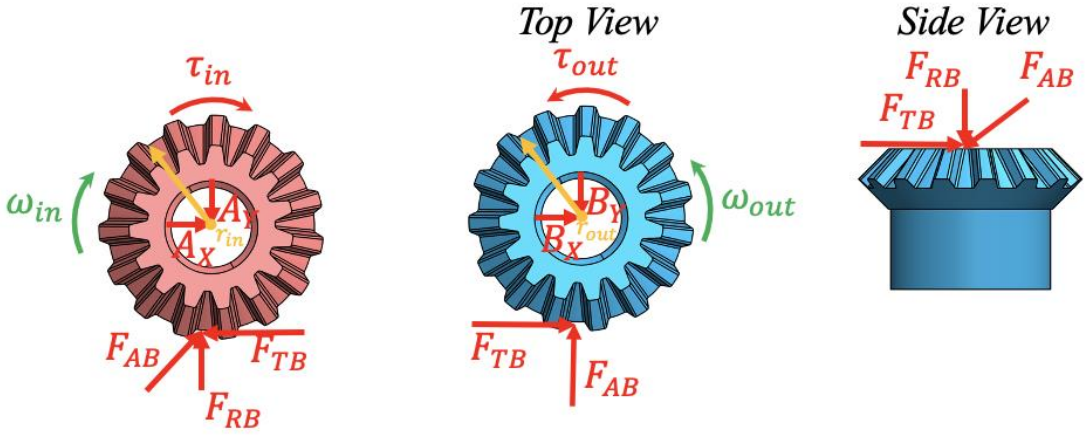

Figure 29: Bevel gear with associated forces demonstrated. The top view and side view are illustrated for clarifying the directional tangential and axial forces present on the system.

Chapter 4 The Proposed Detachable Bronchoscope Design

4.1 Design Overview

To fulfill the medical requirements of a bronchoscope, the design being developed must retain all functionality of an in-use device while also featuring a detachment system. It is a requisite that the device has a control knob to maneuver the distal linkage system of the scope. The distal end must also move smoothly with equal incremental rotation from the control knob to distal end rotation. The insertion section must also allow for accommodated space of a working channel of at least 0.8mm in diameter. Housed on the insertion section must be connective ports that engage to the visualization and illumination component of the bronchoscope. These requirements must fit within the size constraint of a 5.25mm outer diameter insertion section. These current requirements have been in consideration of the design proposed in this thesis. The current model designed using SolidWorks is shown in Figure 29. Many aspects of the model were 3D printed to develop iteratively prototype the design. Using SLA (Stereolithography) technology, the handle, transmission system, and portions of the insertion section were 3D printed. The entire model is shown in Figure 30.

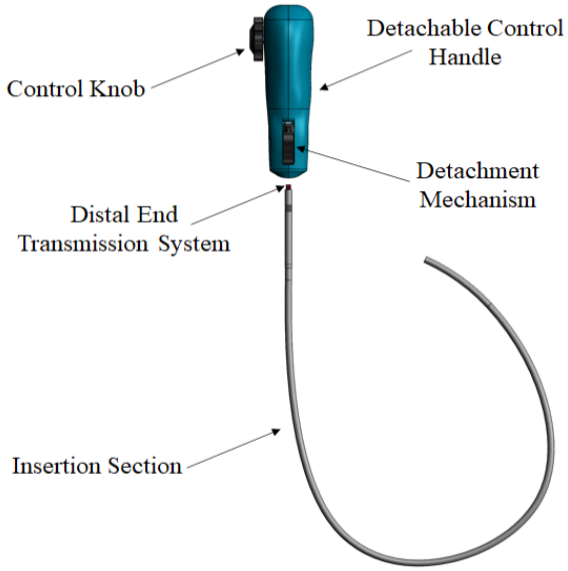

Figure 30: SolidWorks illustration annotated featuring the detachable bronchoscope decoupled

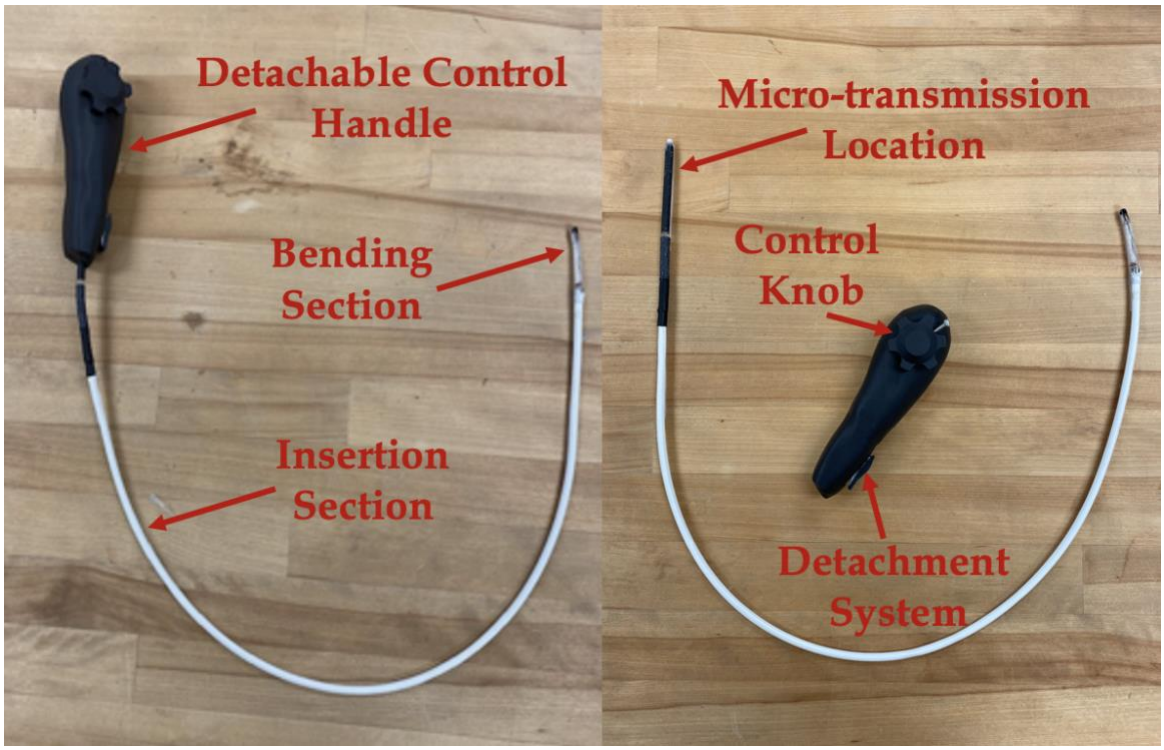

Figure 31: Complete detachable bronchoscope prototype assembled. The handle is attached and shown to the left of the image while the system decoupled is shown on the right

4.1.1 The Detachable Control Handle

There are many design requirements for the handle due to the importance of its direct interaction with the medical practitioner using it. The handle must conform to the user's hand so that it is ergonomic, comfortable, and easy to use. As shown in Figure 32(a), the handle incorporates a sliding mechanism for detachment, a control knob for articulation, and an access point for the bronchoscope insertion section. The handle also must be capable of enclosing the gear box used to translate the control knob rotary motion into the desirable transmission rotary motion. The final handle design was approximately 15 cm in length and cross section diameter of 6 cm. The 3D printed device is shown in Figure 33. Special care was taken to ensure the tolerances allowed for smooth control knob motion and smooth slider mechanism movement for detachment.

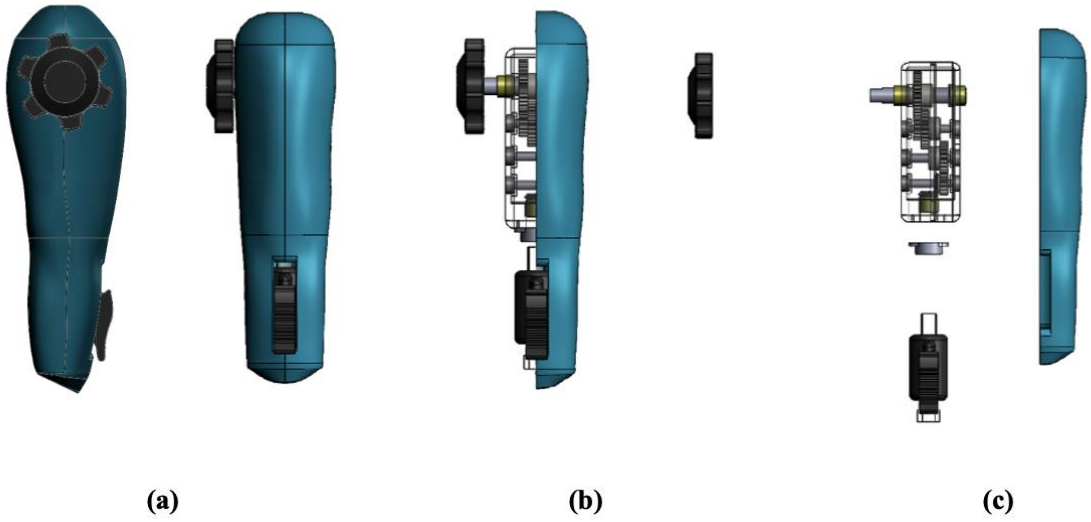

Figure 32: (a) SolidWorks design of detachable bronchoscope handle (b) SolidWorks cross-section view of handle and inner components (c) Exploded SolidWorks cross-section view of handle and inner components

Figure 33: (a) SolidWorks design of detachable bronchoscope handle (b) SolidWorks cross-section view of handle and inner components (c) Exploded SolidWorks cross-section view of handle and inner components

4.1.2 Gearbox

The detachable bronchoscopes distal end is steered by the control knob located on the handle of the device. A gearbox housed inside the handle allows the conversion of a quarter turn to be equivalent to a 20-degree rotation of the distal system. The gearbox, illustrated in Figure 34, is a compounded gearset that contains both spur and bevel gears meshed with a ratio of 1:5. This indicates that the operator will input 1 revolution of the topmost spur year and in effect produces an output of 5 revolutions at the bottom most bevel gear. It is required that the gear system be compact, allowing for a slimmer compartment space inside the control handle. This creates more opportunity for the control handles design to meet an ergonomic standard that is present in all bronchoscopes used in practice. The gearbox must also maintain minimal friction, smooth motion, without the presence of large displacements that may cause bodily harm due to the gearbox having direct control of the linkage system at the distal end. The low friction of the gearbox is managed through the material choice, gear spacing, and the rotation of the rods on the bushings.

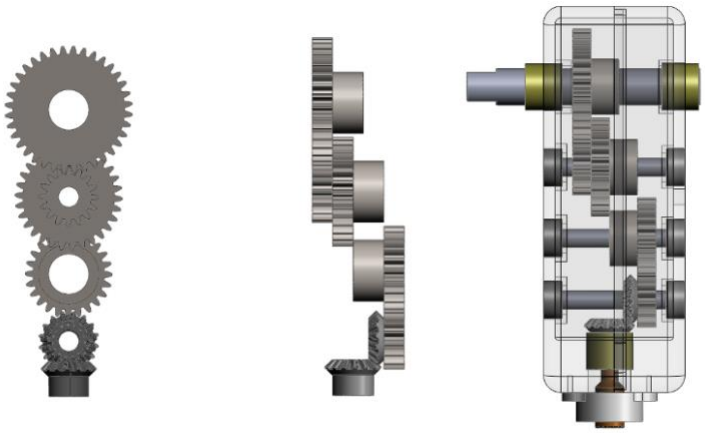

Figure 34: The gearbox of the detachable bronchoscope. A compounded gear system composing of spur gears and bevel gears. The bevel gears on the bottom of the gear transmission allow for the torque transfer direction to change for direct alignment to the micro-transmission mechanism.

4.1.3 The Micro-Transmission

The output of the gearbox controls the motion of a transmission system located in the proximal portion of the detachable bronchoscopes insertion section. This transmission system is a screw joint, with both a right-handed thread and left-handed thread along one shaft. The shaft design allows the conversion from the rotational output of the gearbox to a linear movement along the shaft of the screw. Having both threads along one shaft allows the system to mimic a pulley system, which is the traditional mechanism used in endoscopes used to maneuver the distal end. The behavior of the shaft is clear when the wires connected to the linkage system are displaced with the rotation of the shaft, an illustration of this is shown in Figure 35. Located on the transmission systems shaft are positioning nuts that are designed to connect to the wires. Depending on the direction of rotation on the transmission system the positioning nuts will slide upwards or downwards resulting in a change in angle of the linkage.

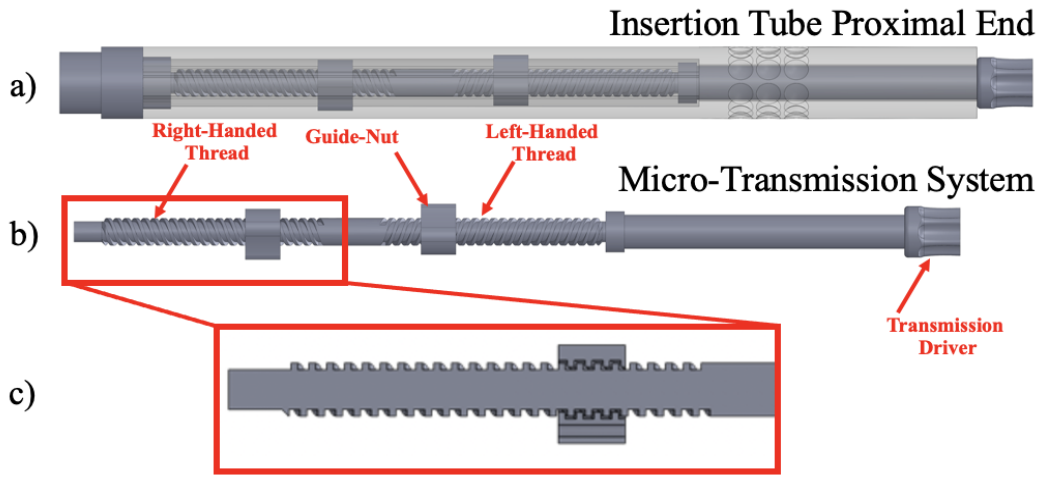

Figure 35: (a) Micro-transmission system with insertion tube proximal end assembly. (b) Annotated micro-transmission system with right-handed thread, left-handed thread, guide-nut with location of input (transmission driver) shown. (c) The screw design cutout shown

To illustrate the drivetrain more closely, it was placed underneath a microscope to visualize. The 3D printed threads of the system can be seen more closely in Figure 36. This shows the 3D printed screw that was developed from stereolithography (SLA) techniques that was used as the micro-transmission system for the detachable bronchoscope.

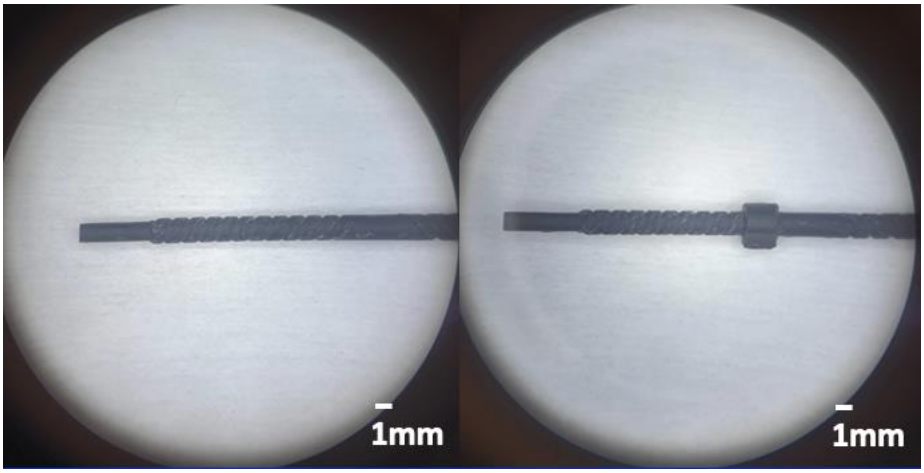

Figure 36: Micro-transmission system depicted under a microscope

4.1.4 The Detachment Mechanism

The detachment system of the detachable bronchoscope enables physicians for quick insertion tube decoupling and recoupling. The system, shown in Figure 37, is placed in the control handle and allows physicians to insert the insertion tubes proximal portion without the thought of orientation due to the designed concave divots placed on the insertion tube. The detachment system engages to divots through the connection of 2mm diameter stainless steel balls. The top view of the placement of the steel balls is illustrated in Figure 38. The balls are

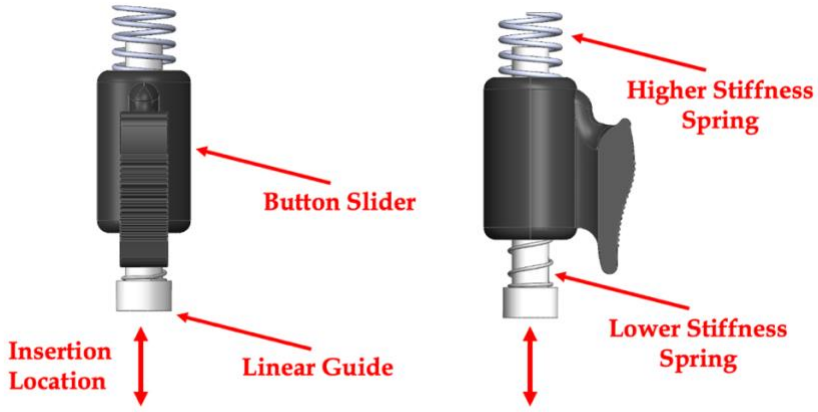

Figure 37: Detachment system showing the button slider and linear guide. The button pushes against the higher stiffness spring to release the system

placed at a separation distance of 120^{o} which allows to securely constraint the insertion tube. To engage the detachment system on the concave divots, the detachment button must be pushed upwards to be placed in an open position. The insertion tube can then be inserted, and the detachment button can then be released. This engages the three ball bearings on the insertion tube. To release, the detachment button is then lifted, and the insertion tube can be removed. The detachment system can be discussed in two separate states called the closed and open state. The

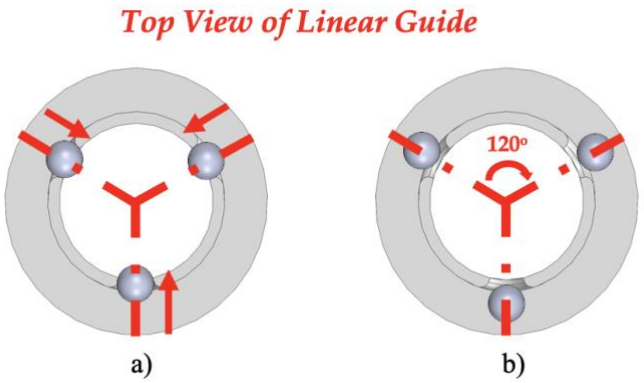

Figure 38: Top of the detachment section cut showing the steel ball separation of the design

closed state of the detachment system is the natural state of the system. The closed state indicates the fixed state that the detachment system is always in. The force from the wall (Figure 39, right), is always present until the button is lifted. When the button is lifted, the system is considered to be in open state, allowing the stainless balls to freely move.

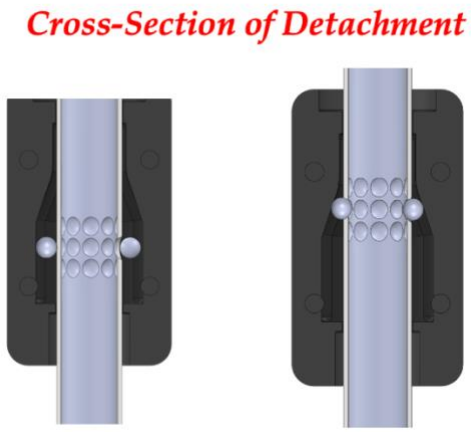

Figure 39: Side view cross section of detachment mechanism shown. The two states are shown. On the left is the open state of the detachment system and on the right is the closed state

Chapter 5 Analytical & Experimental Results

5.1 Micro-Transmission Design

Bronchoscopes are used across a wide range of medical procedures. It is highly desirable for a medical practitioner to have a bronchoscope arm that can detach from and reattach to its handle. The micro-transmission allows for the bronchoscope to detach from and reattach to the insertion arm during a medical procedure, while maintaining control of the articulating distal end. The performance of this micro-transmission system is significant in maneuvering the distal end. In this chapter, the equations calculating the load of the screw design are reviewed and the maximum load of different screw lead arrangements is determined experimentally.

The power screw developed and mentioned in this thesis is capable of producing behaviors comparable to a pulley system that is incorporated in conventional bronchoscopes. The system is entirely 3-D printed and allows manipulation of the distal end through the translation of guide nuts along a single screw axis. The translation of the guide nuts is performed through the input torque on the screw. This system is illustrated in Figure 40 and is composed of a right-handed and left-handed multi-threaded design that is able to transmit the load along the axis of the screw. Square nuts were first designed using SolidWorks, a commercially available computer-aided design (CAD) software, and then manufactured using SLA (Stereolithography) 3D printing technology. The guide nuts illustrated on the transmission system translate linearly and slide against the walls of the insertion tube. The design of the guide nuts friction along the wall is minimized allowing for a stable and smoother translation as the screw system is rotated. As previously mentioned, the right and left-handed are multi-threaded allowing for a larger distance of travel per revolution of

the guide nut. This allows for a quicker mode of travel when the operator is rotating the control knob on the bronchoscope.

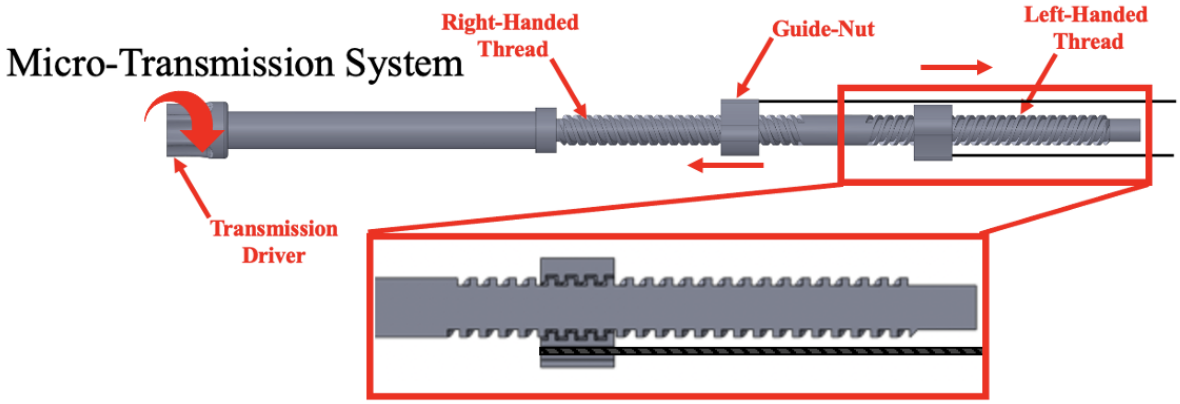

Figure 40: Micro-transmission system with right-handed and left-handed thread. The guide nuts linear movement shown with rotation from on the transmission driver.

5.2 Experimental Setup

For the requirements of the detachable bronchoscope function as a conventional bronchoscope, the materials used, thread design, and design constraints of the micro-transmission system must be considered. This system must also be able to contain and lift an average load of 10N and this was determined by measuring the tension force of a common bronchoscope with a force gauge. To measure load carrying capacity of the micro transmission system, a S-type load cell (Figure 41) was connected directly to the output of the insertion tube. This connection was made from the angulation wire and was directly to the load cell. Although in the experiment there

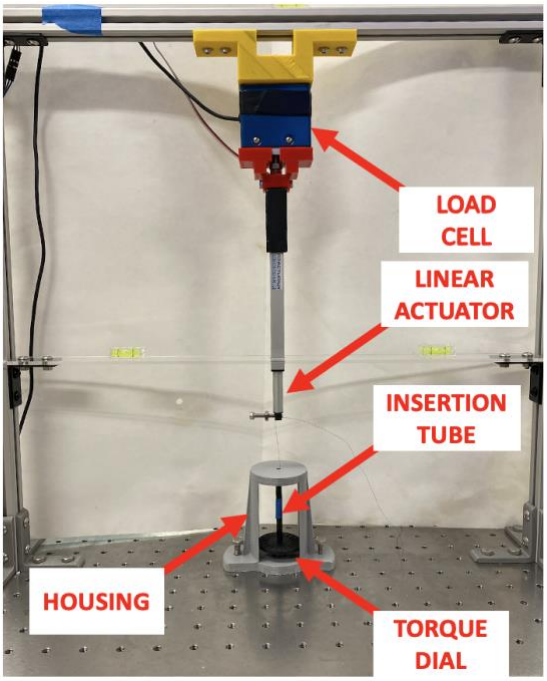

Figure 41: Load cell carrying load benchtop experimental setup

can be stretching of the wire due to constant loading and unloading, it is assumed that this connection will remain taut when the wire is connected to the guide nut. To increase and decrease the loading, a torque dial is rotated causing the guide nut to translate linearly that generates a carrying load that is measured by the loadcell. The insertion tube is assembled in the housing unit that constrains the movement and directly aligned with the axis of the load cell and linear actuator (Figure 41). Located inside of the insertion tube is the 3D printed screw design that is experimentally evaluated. Three separate trials were then conducted with a 2mm and 5mm pitch micro-transmission system that measured there carrying load capacity and their maximum load capabilities.

5.3 Experimental Results and Discussion

In the 2mm pitch screw the maximum load reached was 9.6N, and in the 5mm pitch screw 6.3N. The results demonstrate that constant loading and unloading can stretch the wire causing the maximum load to decrease. This can be adjusted in future experiments by choosing a wire that can

withstand this cycle of loading. This experiment additionally shows that the load ability increases with the decreasing pitch value, a result that can be shown from the carrying load equations derived

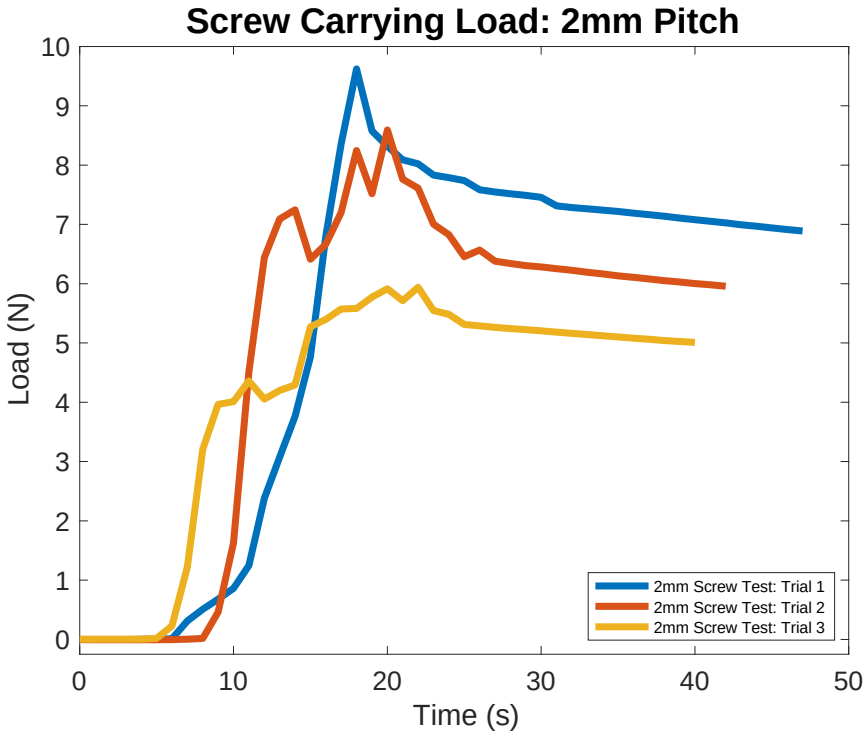

Figure 42: Experimental results from benchtop for a 2mm pitched 3D printed screw

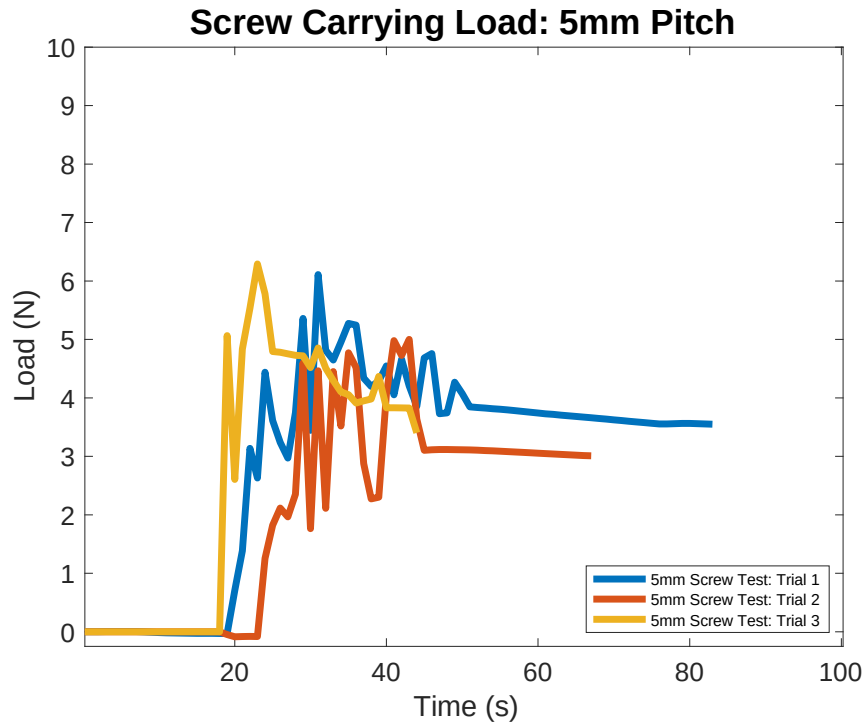

Figure 43: Experimental results from benchtop for a 5mm pitched 3D printed screw

in this thesis. By changing the pitch less than 2mm and material properties of the screw, the requirement of the meeting the average load of 10N can be reached with this transmission system making it an ideal candidate to place inside the detachable bronchoscope prototype.

The experimental results show promising load capacity from 3D printed materials (Figure 42 and Figure 43), with the highest load bearing 10 Newtons. In each trial for the 3D printed screws, there are maximum loads that were reached experimentally. These maximum loads are illustrated on Figure 44 and illustrates that as the pitch decreases, the maximum carrying load increases. This

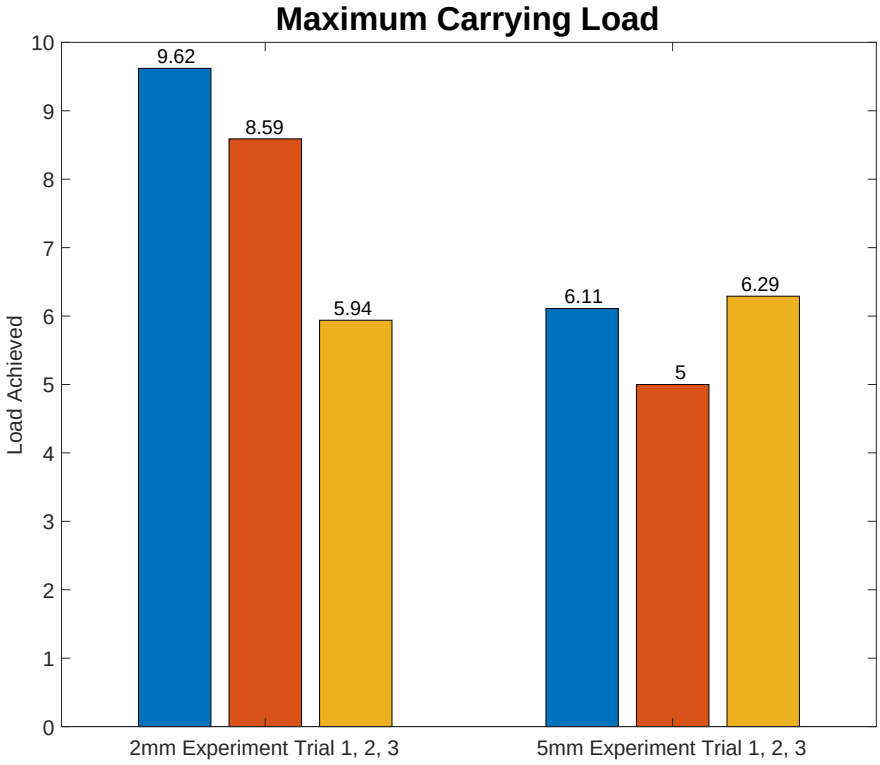

Figure 44: Maximum load characteristics of the screw transmission system

observation can be attributed to two things, radial forces that cause slipping in screws, and a change in part strength. Depending on the design parameters such as lead and thread angle, radial forces, and the angle of the normal force on the thread itself will vary dramatically. In our setup, the thread

diameter, pitch, and number of starts are kept constant while thread width varies. This combination can have an adverse effect on the strength of the nut at larger leads due to the bulk mass removed on the inner threading.

5.4 Summary

A micro-transmission has been proposed for use in a bronchoscope insertion arm so that it can detach and reattach to the handle during medical procedures. The effect of design parameters (i.e., pitch, lead angle, and thread angle) on carrying load was investigated analytically and experimentally. Micro-transmissions with 2mm and 5mm pitches were 3D printed and the maximum carrying load capacity was measured experimentally, at approximately 9 N and 6 N, respectively. The ability to 3D print the screw designs allow for rapid experimentation and verification of the designs.

5.5 Acknowledgements

I would like to thank Professor Frank E. Talke for his support as the chair of my committee. His mentorship, support on my thesis work, and master's education has been significant to the development of this work.

I would also like to thank Dr. Farshad Ahadian, for his insightful outlook on engineering science and his feedback on medical devices. His support was critical in the development of the research conducted throughout this thesis.

I want to acknowledge and thank Professor Karcher Morris. His leadership, and forward thinking is an invaluable asset in a medical device research laboratory.

I would also like to acknowledge Yu Li for his many late nights spent and support on the project, and constant drive to improve the device.

I would also like to thank the rest of the Talke biomedical device laboratory for their research support, perspectives, and feedback. Thank you Rafaela Simones-torigoe, Po-han Chen, Shengfan Hu, Luke Teragan, Allen Hsieh, Benjamin Suen, Oren Gotlib.

Material from this thesis, has been published as it appears in ASME ISPS Design of a 3D Printed Micro-Transmission System for a Detachable Bronchoscope 2021. Kohanfars, Matthew; Li, Yu; Morris, Karcher; Ahadian, Farshad; Talke, Frank.

References

[1] Fletcher, Jenna, and Kevin Martinez. 2020. “Trachea: Everything you need to know,” Medical News Today. https://www.medicalnewstoday.com/articles/trachea.

[2] Wikimedia Commons contributors, "File:Diagram showing a bronchoscopy CRUK 053.svg," *Wikimedia Commons, the free media repository,* https://commons.wikimedia.org/w/index.php?title=File:Diagram_showing_a_bronchoscopy_CRUK_053.svg&oldid=503030989.

[3] Kollmeier, Brett R., Lydia C. Boyette, Gabriel B. Beecham, Ninad M. Desai, and Shailesh Khetarpal. 2021. “Difficult Airway,” *StatPearls [Internet]* (January). Treasure Island (FL). https://www.ncbi.nlm.nih.gov/books/NBK470224/.

[4] O'Brien, Sharon M.. 2016. “Understanding the Mallampati score,” *The Waiting Room* (blog). *Clinical Advisor*, https://www.clinicaladvisor.com/home/the-waiting-room/understanding-the-mallampati-score/.

[5] Sofi, Khalid, and Kariman El-Gammal. 2010. “Endotracheal tube defects: Hidden causes of airway obstruction,” *Saudi journal of anaesthesia*, *4*(2), 108–110. https://doi.org/10.4103/1658-354X.65123.

[6] Panchabhai, Tanmay S., and Atul C. Mehta. 2015. “Historical Perspectives of Bronchoscopy. Connecting the Dots,” Ann Am Thorac Society, 12(5), 631–41. https://doi.org/10.1513/AnnalsATS.201502-089PS.

[7] Becker, Heinrich D.. 2020. “A Short History of Flexible Bronchoscopy,” *Flexible Bronchoscopy, Fourth Edition*, 1-19. https://doi.org/10.1002/9781119389231.ch.

[8] Kurimoto, Noriaki, and Teruomi Miyazawa. 2012. “Bronchoscopy in the New Millennium” *Flexible Bronchoscopy, Third Edition*, 1-5. https://doi.org/10.1002/9781444346428.ch1.

[9] Jacaranda Physics 1 2nd Edition, John Wiley & Sons, Inc.

[10] R. Kohli, Divyanshoo, and John Baillie. 2019. “Clinical Gastrointestinal Endoscopy (Third Edition),” Elsevier, 24-31, https://doi.org/10.1016/B978-0-323-41509-5.00003-7.

[11] OLYMPUS. “Therapeutic Bronchoscope (BF-XT190),” Products, https://medical.olympusamerica.com/products/bronchoscope/therapeutic-bronchoscope-bf-xt190.

[12] AMBU. “AMBU ASCOP 4 BRONCHO REGULAR,” Products, https://www.ambu.com/endoscopy/pulmonology/bronchoscopes/product/ambu-ascope-4-regular.

[13] Verathon. 2020. “GlideScope BFlex Single-Use Flexible Bronchoscopes,” https://www.verathon.com/wp-content/uploads/2020/05/0900-5042_Rev-01_GlideScope_BFlex_Brochure_WEB.pdf

[14] Auris. “Monarch Platform,” Auris Health, https://www.aurishealth.com/monarch-platform

[15] Garbin , Nicolo, Long Wang, James H. Chandler, Keith L. Obstein, Nabil Simaan, and Pietro Valdastri. 2018. "A disposable continuum endoscope using piston-driven parallel bellow actuator," International Symposium on Medical Robotics (ISMR), 1-6, https://doi.org/10.1109/ISMR.2018.8333287.

[16] Chen, Yi, Shigehiko Tanaka, and Ian W. Hunter. 2010. "Disposable endoscope tip actuation design and robotic platform," *Annual International Conference of the IEEE Engineering in Medicine and Biology*, 2279-2282, https://doi.org/10.1109/IEMBS.2010.5627677.

[17] Penumbrainc. 2016. “Big Coil Advantage*,”* Brochure. https://www.penumbrainc.com/wp-content/uploads/2016/12/7283E_PenumbraCoil400_Brochure_USA.pdf.

[18] Marini, Louis J. 1999. “Endoscopic Instrument with Removable Front End”. United States, US6077290A, filed September 10, 1999, and issued June 20, 2000.

[19] Krupa, J. Robert, Thomas V Root, William F. Laflash, Anthony J. Parillo, and Aleksandra A. Levshina. 2008. “Endoscope with Detachable Elongation Portion”, United States, Provisional patent 20080214896, filed January 10, 2008.

[20] Nakaichi, Katsumi, Shinji Yamamori, Hironori Kuroyone, Norio Ishikawa, Kohei Ono, and Hidehiro Hosaka. 1997. “Endoscope with detachable operation unit and insertion unit,” United States, US6004263A, filed March 13, 1997, and issued December 21, 1999.

[21] Lynch, Kevin M., and Frank C. Park. 2017, “Modern Robotics Mechanics, Planning, and Control,” Cambridge University Press.

[22] Ball, Robert Stawell. 2019. “Theory of Screws: A Study in the Dynamics of a Rigid Body,” *Creative Media Partners, LLC*.

[23] In the Loupe. 2017. “Multi-Start Thread Reference Guide,” *Harvey Performance Company,* https://www.harveyperformance.com/in-the-loupe/multi-start-thread-guide/#:~:text=A%20multi%2Dstart%20thread%20consists,increased%20without%20changing%20its%20pitch.

[24] Hollander, Kevin W., and Thomas G. Sugar. 2006. “Design of Lightweight Lead Screw Actuators for Wearable Robotic Applications,” *ASME Journal of Mechanical Design,* 128(3), 644–648, https://doi.org/10.1115/1.2181995.

[25] Marrs, Jennifer. 2011. *Machine Designers Reference*. Pages 666-668. Industrial Press

[26] Shigley, Joseph, Charles Mischke, and Thomas H. Brown. 2004. “Standard Handbook of Machine Design. Ukraine: McGraw-Hill Education,” Edited by Joseph Edward Shigley, Charles R. Mischke, and Thomas H Brown. Ukraine: McGraw-Hill Education.

[27] Boston Gear. “Engineering Information Spur Gears,” https://www.bostongear.com/-/media/Files/Literature/Brand/boston-gear/catalogs/p-1930-bg-sections/p-1930-bg_engineering-info-spur-gears.ashx.

[28] Formlabs White Paper. 2017. “Engineering Fit: Optimizing Design for Functional 3D Printed Assemblies,” *Formlabs*.

[29] Engineering ToolBox. 2004. “Friction and Friction Coefficients,” [online], https://www.engineeringtoolbox.com/friction-coefficients-d_778.html.